Journal of Medicinal Chemistry

Article

Cite This: J. Med. Chem. 2020, 63, 2455−2469

pubs.acs.org/jmc

Distorted Gold(I)−Phosphine Complexes as Antifungal Agents

Emily K. Dennis,[†] Jong Hyun Kim,[‡] Sean Parkin,[‡] Samuel G. Awuah,*[,‡] and Sylvie Garneau-Tsodikova*[,†]

[†]Department of Pharmaceutical Sciences, College of Pharmacy, University of Kentucky, 789 South Limestone Street, Lexington, Kentucky 40536-0596, United States

[‡]Department of Chemistry, College of Arts and Sciences, University of Kentucky, 505 Rose Street, Lexington, Kentucky 40506-0055, United States

Supporting Information

ABSTRACT: Fungi cause serious nosocomial infections including candidiasis and aspergillosis, some of which display reduced susceptibility to current antifungals. Inorganic compounds have been found to be beneficial against various medical ailments but have yet to be applied to fungal infections. Here, we explore the activity of linear and square-planar gold(I)−phosphine complexes against a panel of 28 fungal strains including *Candida* spp., *Cryptococcus* spp., *Aspergillus* spp., and *Fusarium* spp. Notably, two square-planar gold(I) complexes with excellent broad-spectrum activity display potent antifungal effects against strains of *Candida auris*, an emerging multidrug-resistant fungus that presents a serious global health threat. To characterize the biological activity of these gold(I) complexes, we used a series of time−kill studies, cytotoxicity and hemolysis assays, as well as whole-cell uptake and development of resistance studies.

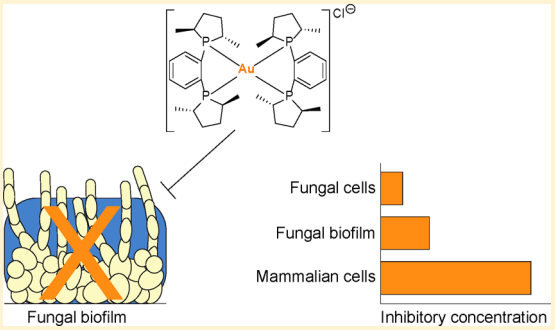

INTRODUCTION

Fungal infections are deadly for patients with conditions that weaken the immune system,[1] as demonstrated by mortality rates exceeding 50% for systemic fungal infections.[2] Those most affected include patients (i) with acquired immune deficiency syndrome, (ii) having received recent chemotherapy, (iii) having had an organ transplant, and (iv) with underlying lung disease such as chronic obstructive pulmonary disorder and asthma.[1,2] These systemic fungal infections are primarily caused by only a few fungal genera, specifically *Candida*[3] and *Aspergillus*.[4]

For treatment of fungal infections, there are three classes of antifungal agents that can be used. One class, the polyenes, includes the widely used antifungal therapy, amphotericin B (AmB). While effective in treating a broad spectrum of infections, treatment is often associated with severe side effects. The second class, the azoles, specifically fluconazole (FLC) and voriconazole (VRC), is a first line of defense against fungal infections but can cause drug−drug interactions. The third class is the echinocandins, which includes caspofungin (CAS). The echinocandins are narrow-spectrum and can only be administered by intravenous catheters. What is of concern is the ability of fungi to be intrinsically resistant to antifungal agents. Examples include *Candida glabrata*[5] to the echinocandins and the emerging pathogen, *Candida auris*, which in some cases is resistant to all three drug classes.[6,7] *C. auris* is currently attracting attention due to recent outbreaks of resistant *C. auris* infections in the U.S.[8−10] In addition, infections can develop decreased susceptibility to antifungal agents during treatment. With a limited armament of antifungal agents, there is a need for new classes of agents.

In agriculture, metal salts (e.g., copper salts[11]) are widely used as fungicides to improve food production. As medicines, inorganic compounds have been predominantly developed as anticancer agents (e.g., cisplatin).[12] These metal complexes typically consist of either platinum, ruthenium, silver, or copper. As anticancer agents, these compounds have been successful but typically have problems with toxicity[13] and associated acquired resistance.[14] More recently gold(I)−phosphine and gold(III) complexes have gained attention as anticancer agents[15] as well as antimicrobials.[16,17]

The arthritis drug, auranofin (Figure 1), is an exemplary gold complex that has been used in the clinic since 1983. It can be administered orally and has been shown to be well-tolerated

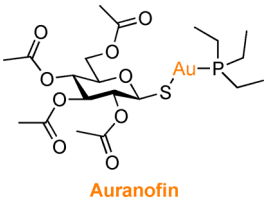

Figure 1. Structure of auranofin.

Special Issue: Women in Medicinal Chemistry

Received: August 30, 2019
Published: December 16, 2019

DOI: 10.1021/acs.jmedchem.9b01436
J. Med. Chem. 2020, 63, 2455−2469

Scheme 1. Synthetic Schemes Showing the Preparation of the Au Complexes 1−6

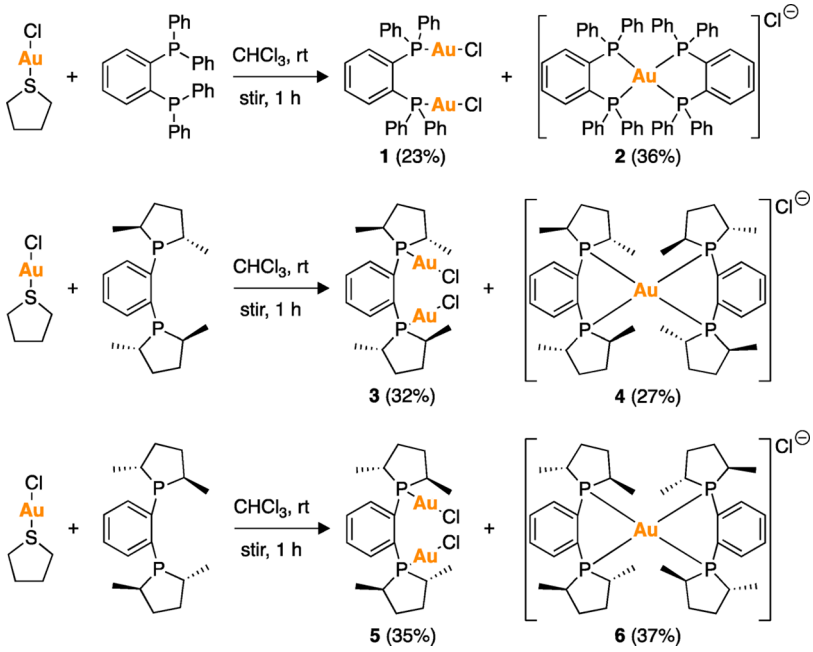

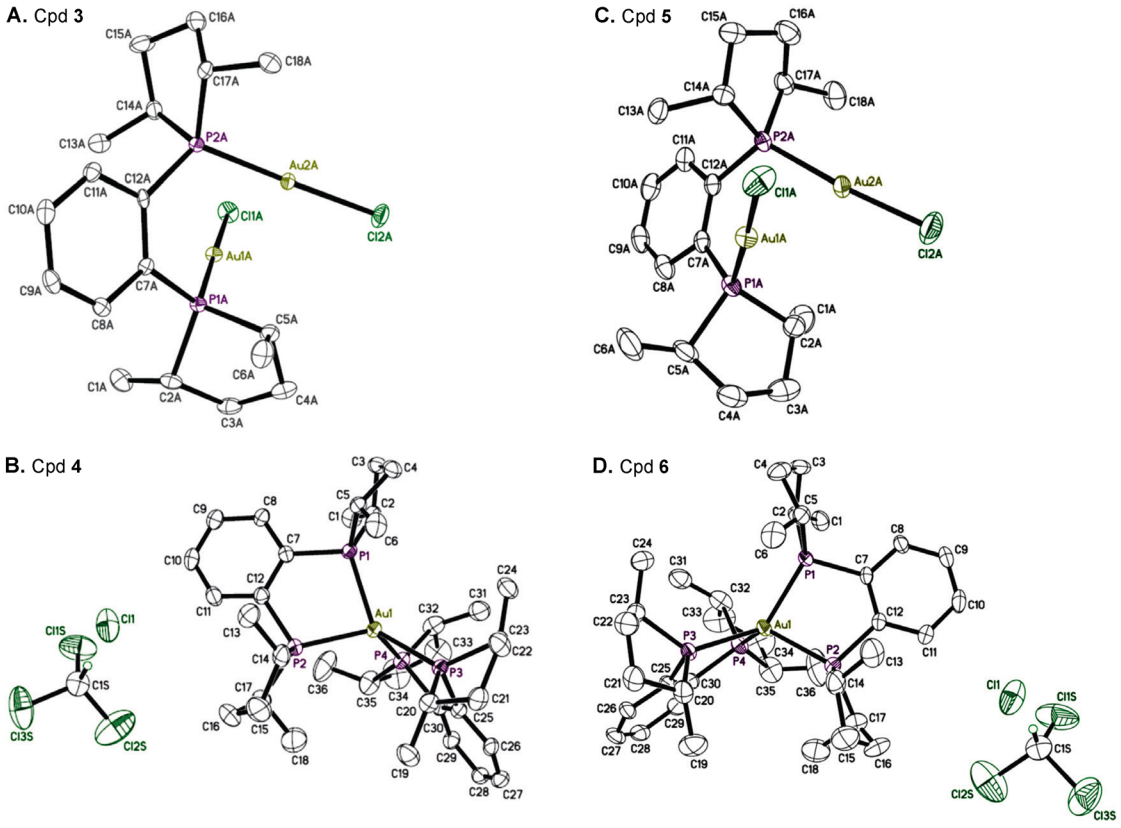

Figure 2. X-ray crystal structures of compounds (A) **3**, (B) **4**, (C) **5**, and (D) **6**. Ellipsoids are drawn at the 50% probability level. Hydrogen atoms bound to carbon atoms are omitted for clarity. For compounds **4** and **6**, the molecules cocrystallized with a molecule of $CHCl_3$.

at a 6 mg daily dose in patients (www.fda.gov/drugsatfda). Auranofin is believed to block inflammation in arthritis by regulating the secretion levels of various cytokines.[18] In recent years, reports looking at repurposing auranofin as an antimicrobial agent against bacteria[19−22] and fungi have been published.[23−26] In fact, auranofin is currently in clinical trials for cancer, HIV, amoebiasis, and tuberculosis.[27,28] As an anticancer and antimicrobial agent, auranofin acts to inhibit thioredoxin reductase.[29,30] With no known inorganic antifungals on the market, auranofin speaks to the promise of using gold scaffolds to investigate and develop novel antifungal agents.

Our group has a long-standing interest in the development of antifungal agents. In the past, we have used different

DOI: 10.1021/acs.jmedchem.9b01436
J. Med. Chem. 2020, 63, 2455−2469

Table 1. MIC Values in μg/mL[a] for Compounds 1−6, Auranofin, and AmB against Various Fungal Strains

		Compound #							
Strains		1	2	3	4	5	6	Auranofin	AmB
Candida albicans	*A*	3.9 (4.3)	15.6 (13.9)	31.3 (40.6)	0.98 (1.2)	3.9 (5.1)	0.49 (0.6)	>31.3 (>46.1)	0.98 (1.1)
	B	15.6 (17.1)	15.6 (13.9)	>31.3 (40.6)	1.95 (2.3)	31.3 (40.6)	0.98 (1.2)	>31.3 (>46.1)	1.95 (2.1)
	C	0.49 (0.5)	15.6 (13.9)	>31.3 (40.6)	0.98 (1.2)	15.6 (20.2)	0.98 (1.2)	>31.3 (>46.1)	3.9 (4.2)
	D	7.8 (8.6)	7.8 (6.9)	31.3 (40.6)	0.98 (1.2)	7.8 (10.1)	0.49 (0.6)	>31.3 (>46.1)	7.8 (8.4)
	E	7.8 (8.6)	7.8 (6.9)	31.3 (40.6)	0.98 (1.2)	15.6 (20.2)	0.49 (0.6)	>31.3 (>46.1)	3.9 (4.2)
	F	7.8 (8.6)	7.8 (6.9)	31.3 (40.6)	0.98 (1.2)	15.6 (20.2)	0.49 (0.6)	>31.3 (>46.1)	3.9 (4.2)
	G	7.8 (8.6)	7.8 (6.9)	31.3 (40.6)	0.98 (1.2)	7.8 (10.1)	0.49 (0.6)	>31.3 (>46.1)	0.98 (1.1)
Non-*albicans Candida*	*H*	7.8 (8.6)	7.8 (6.9)	>31.3 (>40.6)	1.95 (2.3)	15.6 (20.2)	0.98 (1.2)	>31.3 (>46.1)	3.9 (4.2)
	I	15.6 (17.1)	15.6 (13.9)	>31.3 (>40.6)	1.95 (2.3)	31.3 (40.6)	0.98 (1.2)	31.3 (46.1)	3.9 (4.2)
	J	15.6 (17.1)	7.8 (6.9)	>31.3 (>40.6)	0.98 (1.2)	15.6 (20.2)	0.49 (0.6)	>31.3 (>46.1)	3.9 (4.2)
	K	>31.3 (>34.3)	>31.3 (>27.8)	>31.3 (>40.6)	3.9 (4.6)	>31.3 (>40.6)	1.95 (2.3)	>31.3 (>46.1)	1.95 (2.1)
	L	>31.3 (>34.3)	>31.3 (>27.8)	>31.3 (>40.6)	7.8 (9.2)	>31.3 (>40.6)	1.95 (2.3)	>31.3 (>46.1)	1.95 (2.1)
Cryptococcus	*M*	0.98 (1.1)	3.9 (3.5)	1.95 (2.5)	0.98 (1.2)	0.12 (0.2)	0.25 (0.3)	≤0.06 (≤0.1)	>31.3 (>33.9)
	N	3.9 (4.3)	3.9 (3.5)	>31.3 (>40.6)	0.98 (1.2)	15.6 (20.2)	0.49 (0.6)	3.9 (5.7)	0.98 (1.1)
	O	3.9 (4.3)	3.9 (3.5)	31.3 (40.6)	0.98 (1.2)	7.8 (10.1)	0.49 (0.6)	7.8 (11.5)	1.95 (2.1)
	P	15.6 (17.1)	3.9 (3.5)	>31.3 (>40.6)	0.98 (1.2)	7.8 (10.1)	0.49 (0.6)	3.9 (5.7)	0.98 (1.1)
Aspergillus	*Q*	>31.3 (>34.3)	>31.3 (>27.8)	>31.3 (>40.6)	3.9 (4.6)	>31.3 (>40.6)	3.9 (4.6)	3.9 (5.7)	15.6 (16.9)
	R	>31.3 (>34.3)	>31.3 (>27.8)	>31.3 (>40.6)	1.95 (2.3)	>31.3 (>40.6)	3.9 (4.6)	7.8 (11.5)	7.8 (8.4)
	S	>31.3 (>34.3)	>31.3 (>27.8)	>31.3 (>40.6)	7.8 (9.2)	>31.3 (>40.6)	7.8 (9.2)	>31.3 (>46.1)	31.3 (33.8)
Fusarium	*T*	>31.3 (>34.3)	31.3 (27.8)	>31.3 (>40.6)	3.9 (4.6)	>31.3 (>40.6)	3.9 (4.6)	>31.3 (>46.1)	7.8 (8.4)

***Candida albicans* strains:** *A* = *C. albicans* ATCC MYA-1003(R), *B* = *C. albicans* ATCC 10231(R), *C* = *C. albicans* ATCC MYA-1237(R), *D* = *C. albicans* ATCC MYA-2310(S), *E* = *C. albicans* ATCC MYA-2876(S), *F* = *C. albicans* ATCC 64124(R), *G* = *C. albicans* ATCC 90819(R). NOTE: (S) and (R) are indicating strains that are reported to be sensitive (S) and resistant (R) to fluconazole by the ATCC.
Non-*albicans Candida* strains: *H* = *C. glabrata* ATCC 2001, *I* = *C. krusei* ATCC 6258, *J* = *C. parapsilosis* ATCC 22019, *K* = *C. auris* AR bank no. 0384, *L* = *C. auris* AR bank no. 0390.
***Cryptococcus* strains:** *M* = *C. neoformans* ATCC MYA-85, *N* = *C. neoformans* CN1, *O* = *C. neoformans* CN2, *P* = *C. neoformans* CN3.
***Aspergillus* strains:** *Q* = *A. nidulans* ATCC 38163, *R* = *A. terreus* ATCC MYA-3633, *S* = *A. flavus* ATCC MYA-3631.
***Fusarium* strain:** *T* = *F. graminearum* 053.
Abbreviations: AmB = amphotericin B; MIC = minimum inhibitory concentration.

MIC ≤1.95 μg/mL (excellent antifungal activity)
MIC = 3.9 - 7.8 μg/mL (good antifungal activity)
MIC ≥15.6 μg/mL (poor antifungal activity)

[a]MIC values are also provided in μM in parentheses.

strategies to develop antifungals, including the development of azole analogues,[31−33] combinations of antifungal drugs,[34−36] and synthesis and biological evaluation of new scaffolds.[37−41] We previously developed gold complexes as potential anticancer agents.[42,43] We were intrigued to see if the applications of gold complexes could be expanded to include antifungal activity. Herein, we present the antifungal activity of six distorted gold(I)−phosphine complexes, **1**−**6** (Scheme 1), not derived or related in structure to auranofin, against yeast, molds, and yeast biofilms. We then confirm the activity of the two best complexes, **4** and **6**, in time−kill studies. To evaluate the efficacy of complexes **4** and **6**, we use both cytotoxicity studies against four mammalian cell lines as well as hemolysis assay with both murine and human red blood cells. We also present whole-cell uptake assays and development of resistance studies. The gold complexes with square-planar geometry appear to show great promise for future development as antifungal agents. As there are currently no metal complexes that have been thoroughly investigated for antifungal activity, our distorted gold(I)−phosphine complexes are innovative in the field of antifungal development.

RESULTS AND DISCUSSION

Design, Chemical Synthesis, and X-ray Crystallography. For this study we wanted to create gold(I) complexes that could be easily prepared in a single synthetic step (Scheme 1). The reaction of three commercially available phosphorus ligands with AuCl(THT) (prepared by the reaction of tetrahydrothiophene and tetrachloroauric acid ($HAuCl_4 \bullet 3H_2O$))[44] in chloroform at room temperature afforded mixtures of linear gold(I) complexes **1**, **3**, and **5** and their square-planar gold(I) complex counterparts **2**, **4**, and **6** in 23−37% yield, which could be easily separated by silica gel flash chromatography. To expand the availability of chiral gold(I) complexes, which are limited and underexplored for biological applications, we used both the achiral bis(diphenylphosphino)benzene ligand and chiral ligands such as the 1,2-bis[(2*S*,5*S*)-2,5-dimethylphospholano]benzene and 1,2-bis[(2*R*,5*R*)-2,5-dimethylphospholano]benzene. The structures of compounds **1**−**6** were confirmed by ^{1}H, ^{13}C, and ^{31}P NMR spectroscopy, mass spectrometry, as well as RP-HPLC for purity determination. Additionally, the structures of compounds **3**, **4**, **5**, and **6** were confirmed by X-ray crystallography. Single crystals of complexes were grown by

DOI: 10.1021/acs.jmedchem.9b01436
J. Med. Chem. 2020, 63, 2455−2469

Table 2. MIC Values in μg/mL[a] for Compounds 4, 6, AmB, CAS, FLC, and VRC against a Panel of *C. auris* Strains

	Compound #					
Strains	**4**	**6**	AmB	CAS	FLC†	VRC†
I	0.98 (1.2)	0.98 (1.2)	1.95 (2.1)	<0.98 (<0.9)	0.49 (1.6)	0.06 (0.2)
II	1.95 (2.3)	0.98 (1.2)	0.98 (1.1)	<0.98 (<0.9)	0.49 (1.6)	0.06 (0.2)
III	1.95 (2.3)	3.9 (4.6)	1.95 (2.1)	1.95 (1.8)	62.5 (204.1)	1.95 (5.6)
IV	1.95 (2.3)	1.95 (2.3)	1.95 (2.1)	<0.98 (<0.9)	>62.5 (>204.1)	3.9 (11.2)
V	1.95 (2.3)	3.9 (4.6)	1.95 (2.1)	7.8 (7.1)	>62.5 (>204.1)	3.9 (11.2)
VI	1.95 (2.3)	1.95 (2.3)	1.95 (2.1)	31.3 (28.6)	0.98 (3.2)	0.06 (0.2)
VII	1.95 (2.3)	1.95 (2.3)	1.95 (2.1)	31.3 (28.6)	>62.5 (>204.1)	0.49 (1.4)
VIII	1.95 (2.3)	1.95 (2.3)	1.95 (2.1)	7.8 (7.1)	>62.5 (>204.1)	0.98 (2.8)
*K**	3.9 (4.6)	1.95 (2.3)	1.95 (2.1)	1.95 (1.8)	31.3 (102.2)	0.24 (0.7)
*L**	7.8 (9.2)	1.95 (2.3)	1.95 (2.1)	7.8 (7.1)	>62.5 (>204.1)	0.49 (1.4)

***C. auris* strains:** I = *C. auris* AR bank no. 0381, II = *C. auris* AR bank no. 0382, III = *C. auris* AR bank no. 0383, IV = *C. auris* AR bank no. 0385, V = *C. auris* AR bank no. 0386, VI = *C. auris* AR bank no. 0387, VII = *C. auris* AR bank no. 0388, VIII = *C. auris* AR bank no. 0389, *K* = *C. auris* AR bank no. 0384, *L* = *C. auris* AR bank no. 0390.

Abbreviations: AmB = amphotericin B; CAS = caspofungin; FLC = fluconazole; MIC = minimum inhibitory concentration; VRC = voriconazole.

*Note: values presented for strains *K* and *L*, which are new to this manuscript, are also presented in Table 1, but are also displayed here for ease of comparison.

†MIC-2 values are presented for azoles. MIC-0 values are presented for all other compounds.

MIC ≤1.95 μg/mL (excellent antifungal activity)

MIC = 3.9 - 7.8 μg/mL (good antifungal activity)

MIC ≥15.6 μg/mL (poor antifungal activity)

[a]MIC values are also provided in μM in parentheses.

vapor diffusion (Figure 2). Crystal structures for the known compounds **1**[45] and **2**[46] had already been solved. The structures of complexes **3** and **5** were consistent with linear geometry for classical gold(I) complexes. Furthermore, complexes **4** and **6** were characterized by a distorted square-planar arrangement around the gold(I) center as observed in gold complexes with bisphosphine ligands. In all cases, the gold(I) center is coordinated to bidentate ligands with phosphorus donors; **3** and **5** have one chloride ion bound to the gold(I) center, while **4** and **6** have all donors as phosphorus atoms. Typically, Au−P distances vary from 2.229 to 2.239 Å and Au−Cl distances are in the range of 2.286−2.292 Å.

Determination of Minimum Inhibitory Concentration (MIC) Values of Compounds 1−6 against 28 Fungal Strains. For all biological studies, we used auranofin as a control as it is one of the only metal complexes that is an FDA-approved drug, is well-tolerated in patients, has some reported antimicrobial activity, and may have a similar cellular target as the gold(I)−phosphine complexes. As there are currently no metal complexes that have been thoroughly investigated for antifungal activity, our distorted gold(I)−phosphine complexes are innovative in the field of antifungal development. For most biological assays, we also used the current FDA-approved antifungal AmB as a positive control.

Compounds **1−6** were first tested in MIC value determination assays against a panel of 20 fungal strains (Table 1). The panel consisted of seven *Candida albicans* (strains *A*−*G*), five non-*albicans Candida* (one *C. glabrata* (strain *H*), one *C. krusei* (strain *I*), one *C. parapsilosis* (strain *J*), and two *C. auris* (strains *K* and *L*)), four *Cryptococcus neoformans* (strains *M*−*P*), three *Aspergillus* (strains *Q*−*S*), as well as one *Fusarium graminearum* (strain *T*). These strains were chosen as they represent pathogens causing systemic infections. Furthermore, this panel includes many (five out of seven) *C. albicans* strains designated as FLC-resistant by the American Type Culture Collection (ATCC, see legend of Table 1). We observed that auranofin had no antifungal activity against *Candida* spp., while it displayed MIC values of 0.06−7.8 μg/mL against all four *C. neoformans* and two of the three *Aspergillus* strains tested, which agrees with other reports of its activity.[24] We found that compounds **4** and **6** displayed excellent activity against *Candida* spp. and *Cryptococcus* spp. with MIC values against 17 strains in the range of 0.06−1.95 μg/mL, which were generally better than MIC values for AmB. Compounds **4** and **6** also displayed good to excellent activity (MIC values of 1.95−7.8 μg/mL) against all filamentous fungi, the *Aspergillus* spp. and *Fusarium* spp., which was much better than that of AmB (MIC values of 7.8−31.3 μg/mL). Compound **3**, on the other hand, was found to be completely inactive against all fungal strains tested except for *C. neoformans* (strain *M*). Compounds **1**, **2**, and **5** were inactive against both *Aspergillus* spp. and *Fusarium* spp. and most of the non-*albicans Candida* strains tested, whereas they displayed some activity in the range of 0.12−7.8 μg/mL against a few strains of *C. albicans* and *C. neoformans*. From these data, we concluded that linear gold(I) complexes (i.e., **1**, **3**, and **5**) and achiral square-planar gold(I) complexes (i.e., **2**) were poor antifungals that should not be further pursued, whereas the chiral square-planar gold(I) complexes (i.e., **4** and **6**) showed great promise as antifungals and deserved further investigation.

As *C. auris* is an emerging drug-resistant pathogen, we included two *C. auris* strains in our initial panel (strains *K* and *L*) (Table 1). As compounds **4** and **6** displayed good and excellent activity against these two *C. auris* strains, respectively, we expanded our panel and tested compounds **4** and **6** as well as the control antifungals AmB, CAS, FLC, and VRC with an additional eight *C. auris* strains (strains I−VIII) from the

DOI: 10.1021/acs.jmedchem.9b01436
J. Med. Chem. 2020, 63, 2455−2469

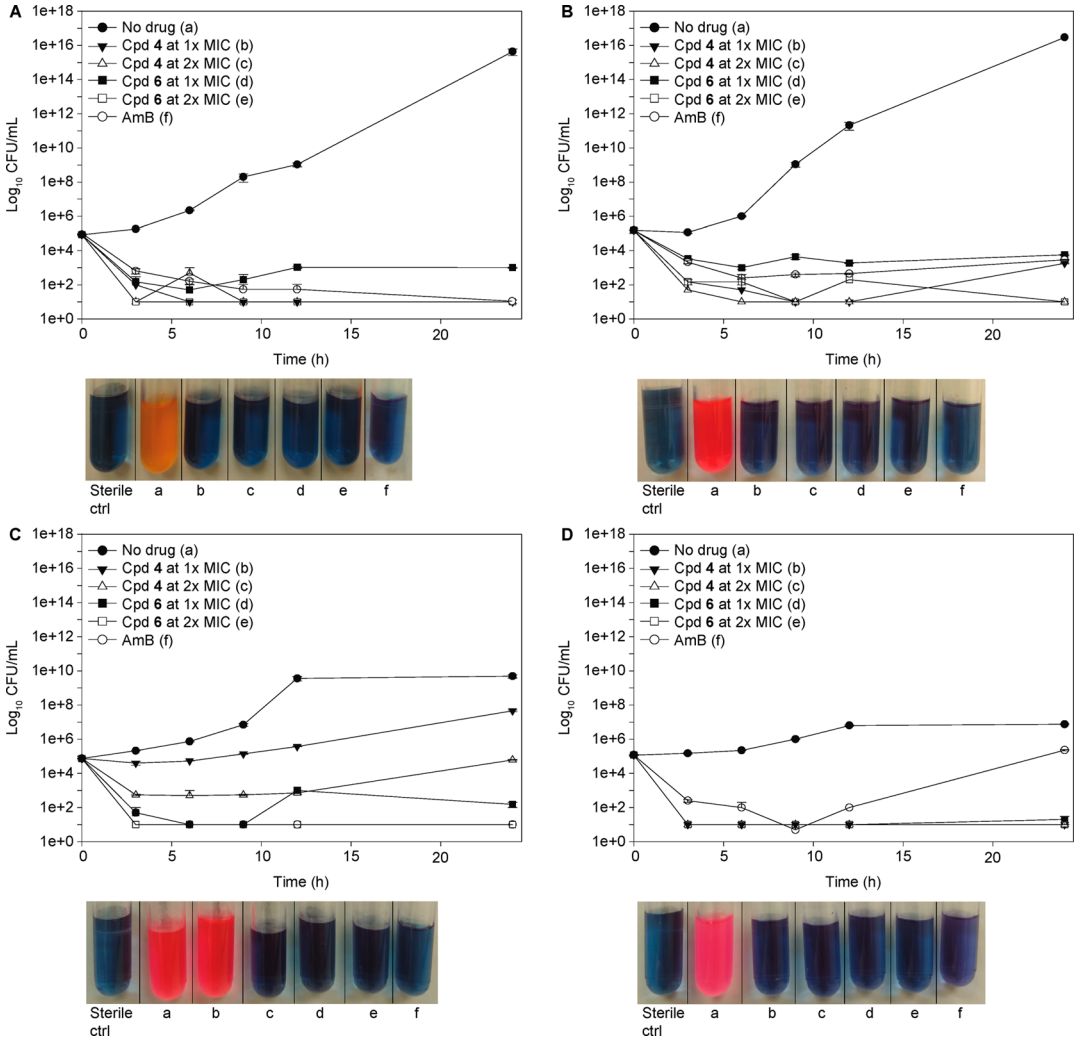

Figure 3. Representative time−kill curves for compounds **4**, **6**, and AmB against (A) *C. albicans* ATCC 10231 (strain *B*), (B) *C. glabrata* ATCC 2001 (strain *H*), (C) *C. auris* AR bank no. 0384 (strain *K*), and (D) *C. auris* AR bank no. 0390 (strain *L*). Fungal strains were treated with no drug (black circles), compound **4** at 1× MIC (inverted black triangle), compound **4** at 2× MIC (white triangle), compound **6** at 1× MIC (black square), compound **6** at 2× MIC (white square), and AmB at 1× MIC (white circle). At the 24-h endpoint, resazurin was added to the cultures to qualitatively measure the CFU/mL. Resazurin, which is a blue-purple color, is metabolized by viable cells to produce resorufin, which has a pink-orange color. Cultures with little to no cells remain a blue-purple color, while dense cultures appear pink or orange.

Centers for Disease Control (CDC) Antibiotic Resistance Bank[47] (Table 2). We observed that both compounds **4** and **6** had excellent antifungal activity (MIC values of 0.98−1.95 μg/mL) against almost all *C. auris* strains.

Time−Kill Assays for Compounds 4 and 6. With the very promising antifungal activity results for compounds **4** and **6**, we next examined their killing kinetics. Time−kill assays were done with four representative *Candida* strains, one *C. albicans* (strain *B*), one *C. glabrata* (strain *H*), and two *C. auris* (strains *K* and *L*) (Figure 3). Compounds **4** and **6** were tested at both their 1× and 2× MIC values, and AmB at 1× MIC was used as a known fungicidal control. Both compounds significantly decreased fungal colony forming units (CFU) by 10^2 CFU/mL by the 3 h time point and did not increase over the 24 h time period, which indicated that compounds **4** and **6** are fungicidal. This pattern was very similar to AmB. With *C. albicans* (strain *B*), compound **4** at 1× MIC reached the limit of detection at 9 h and compound **6** at 2× MIC at 3 h. With *C. glabrata* (strain *H*), both compounds at 2× MIC were at the limit of detection by 24 h. For *C. auris* (strain *K*), compound **4** failed to reach the limit of detection by 24 h, but compound **6** at 1× MIC reached the limit at 6 h. However, with *C. auris* (strain *L*) both compounds **4** and **6** at 1× MIC reached the limit of detection by 3 h and remained under the limit of detection, while AmB reached the limit of detection at 9 h before the CFU/mL began to return to the original yeast cell concentration.

Prevention of Biofilm Formation and Disruption of Preformed Biofilm Assays for Compounds 4 and 6. Biofilms are well-known in the world of bacteria to cause difficult to treat and reoccurring infections by a multitude of species including *Staphylococcus aureus*, *Escherichia coli*, and *Pseudomonas aeruginosa*.[48,49] There is an extensive number of fungal strains known to form biofilms, but biofilm formation on catheters, prostheses, and other medical devices in healthcare associated infections is mainly limited to *Candida* spp.[50−53] The ability of compounds **4** and **6** to both prevent and disrupt biofilm formation is important for prophylactic treatment and to stop the spread of a fungal infection. However, it is regarded that it is more challenging to disrupt a

DOI: 10.1021/acs.jmedchem.9b01436
J. Med. Chem. 2020, 63, 2455−2469

preformed biofilm as the large, sugary extracellular matrix that is the key characteristic of biofilms can prevent many drugs from reaching the fungal cells.[54] Furthermore, in biofilms, fungal cells can upregulate efflux pumps to prevent the action of any drugs that do reach the fungal cells through the extracellular matrix.[55] We measured the ability of compounds **4** and **6**, auranofin, and AmB both to prevent biofilm formation and to disrupt preformed biofilms of *C. albicans* (strain *B*), *C. glabrata* (strain *H*), and *C. auris* (strains *K* and *L*) (Table 3 and Figures S31 and S32). As the biofilm assay is a colorimetric assay and it is difficult to achieve 100% disruption of biofilms, we report the sessile MIC_{90} ($SMIC_{90}$), which is the concentration of compound at which there is a 90% decrease in metabolic activity as compared to untreated biofilm. Both compounds **4** and **6** showed similar results with all four fungal strains tested. $SMIC_{90}$ values in prevention of biofilm formation assays were 1- to 2-fold higher than with planktonic cells. When tested against a preformed biofilm, compound **4** had a $SMIC_{90}$ of 7.8−15.6 μg/mL with all four strains and compound **6** had a $SMIC_{90}$ of 3.9−7.8 μg/mL with all four strains. These $SMIC_{90}$ results were 4- to 8-fold higher than the MIC results for the same *Candida* strains with planktonic cells. Interestingly, auranofin with *C. albicans* (strain *B*) achieved the same $SMIC_{90}$ as compound **4** but was inactive against *C. glabrata* (strain *H*) and the two *C. auris* (strains *K* and *L*) tested. These values for auranofin are similar to a value reported for auranofin against the biofilm of one *C. albicans* strain.[23] In contrast, AmB had $SMIC_{90}$ values of 1.95 μg/mL (*C. auris*, strain *K*) 7.8 μg/mL (*C. auris*, strain *L*; *C. glabrata*, strain *H*), and 31.3 μg/mL (*C. albicans*, strain *B*), which were 1- and 16-fold higher than its MIC values against the same strains in liquid culture.

It is promising that both compounds **4** and **6** have good activity against biofilms of *Candida* spp. There have been reports that compared planktonic and sessile MIC values of other FDA-approved antifungal agents, which demonstrate the reduced susceptibility of biofilms to antifungal agents.[52,56] Of the currently used antifungal agents, AmB and echinocandins have the best efficacy with biofilms with $SMIC_{90}$ in the range of 0.5−128 μg/mL (4- to 128-fold increase from MIC) and 0.03−8 μg/mL (2- to 16-fold increase from MIC), respectively. For the azoles, itraconazole and posaconazole have some efficacy against biofilms with 1- to 256-fold increases in MIC against biofilms. However, VRC and FLC have no efficacy with $SMIC_{90}$ exceeding 512 μg/mL. Additionally, new investigational antifungal molecules that have been reported to be active against *C. albicans* biofilms include azole derivatives and benzimidazole containing compounds. For the azole derivatives, seven econazole derivatives were reported with minimum biofilm inhibiting concentrations at or near 8 μg/mL[57] (2- to 16-fold increase in MIC) and alkylated azole derivatives displayed $SMIC_{80}$ values of 15.6−31.3 μg/mL.[32] Other investigational molecules with activity against biofilms included three neomycin B−benzimidazole hybrid molecules with $SMIC_{80}$ values of 7.8−15.6 μg/mL[32,58] (2- to 4-fold increase in MIC). *Candida* biofilms are known to be key virulence factors in mucosal membrane infections (i.e., thrush and vulvovaginal infections),[59−61] and *Candida* clinical isolates from bloodstream infections can form biofilms as well. Of the bloodstream isolates, it is estimated that approximately 20% of *C. albicans* strains were able to form biofilm *in vitro*, with that percentage increasing to near 70% for non-*albicans* *Candida*.[62−64] With few other antifungals displaying antibiofilm activity, the 4-fold difference that we observed is highly promising.

Table 3. Prevention of Biofilm Formation and Disruption of a Preformed Biofilm by Compounds 4, 6, Auranofin, and AmB against Four Fungal Strains[a]

strain	compd	biofilm prevention $SMIC_{90}$ (μg/mL)	preformed biofilm $SMIC_{90}$ (μg/mL)
B	**4**	3.9	7.8
	6	0.98	3.9
	auranofin	7.8	7.8
	AmB	0.98	31.3
H	**4**	3.9	7.8
	6	1.95	3.9
	auranofin	31.3	>31.3
	AmB	0.98	7.8
K	**4**	3.9	7.8
	6	3.9	7.8
	auranofin	>31.3	>31.3
	AmB	1.95	1.95
L	**4**	3.9	15.6
	6	3.9	7.8
	auranofin	>31.3	>31.3
	AmB	1.95	7.8

[a]Strains: *B* = *C. albicans* ATCC 10231, *H* = *C. glabrata* ATCC 2001, *K* = *C. auris* AR bank no. 0384, *L* = *C. auris* AR bank no. 0390.

Mammalian Cytotoxicity Assays for Compounds 4 and 6. For the gold complexes to progress further into the drug development process, the gold complex activity should be specific to fungal cells and not be toxic to mammalian cells. Therefore, we tested compounds **4** and **6** as well as the control auranofin against four mammalian cell lines: human adenocarcinoma (A549), bronchial epithelial (BEAS-2B), human embryonic kidney (HEK-293), and murine macrophage (J774A.1) (Table 4, Figure 4). Excluding auranofin with J774A.1, we observed <50% cell survival at 7.8 μg/mL with no cell survival at 15.6 μg/mL for both compounds **4** and **6** and auranofin. Auranofin displayed IC_{50} values of 0.5−3.0 μM against A549, BEAS-2B, and HEK-293 cell lines, which agrees with other published values against cisplatin-sensitive cell lines.[42] For J774A.1, the IC_{50} value for auranofin was significantly higher at 16.2 μM. As J774A.1 is a macrophage cell line, auranofin may have had an anti-inflammatory effect that stimulated cell metabolism, which could account for the higher IC_{50} value. There is interest in repurposing auranofin as an antimicrobial; however, auranofin does not appear to be promising as an antifungal. Auranofin displayed poor activity against *Candida* spp. (MIC > 31.3 μg/mL) and only good activity against two *Aspergillus* spp. (MIC = 3.9 and 7.8 μg/mL). For compound **4**, IC_{50} values were very similar for BEAS-2B, HEK-293, and J774A.1 (1.5−2.0 μM) and somewhat higher for A549 (4.5 μM). The MIC values for compounds **4** and **6** against 18 of the *Candida* spp. are in the range of 0.49−

Table 4. IC_{50} (μM) for Mammalian Cell Lines

compd	A549	BEAS-2B	HEK-293	J774A.1
4	4.5 ± 0.6	2.0 ± 0.3	1.9 ± 0.7	1.5 ± 0.1
6	2.5 ± 0.2	4.9 ± 0.3	5.7 ± 0.5	1.5 ± 0.1
auranofin	0.5 ± 0.1	1.3 ± 0.1	3.0 ± 0.2	16.2 ± 0.9

DOI: 10.1021/acs.jmedchem.9b01436
J. Med. Chem. 2020, 63, 2455−2469

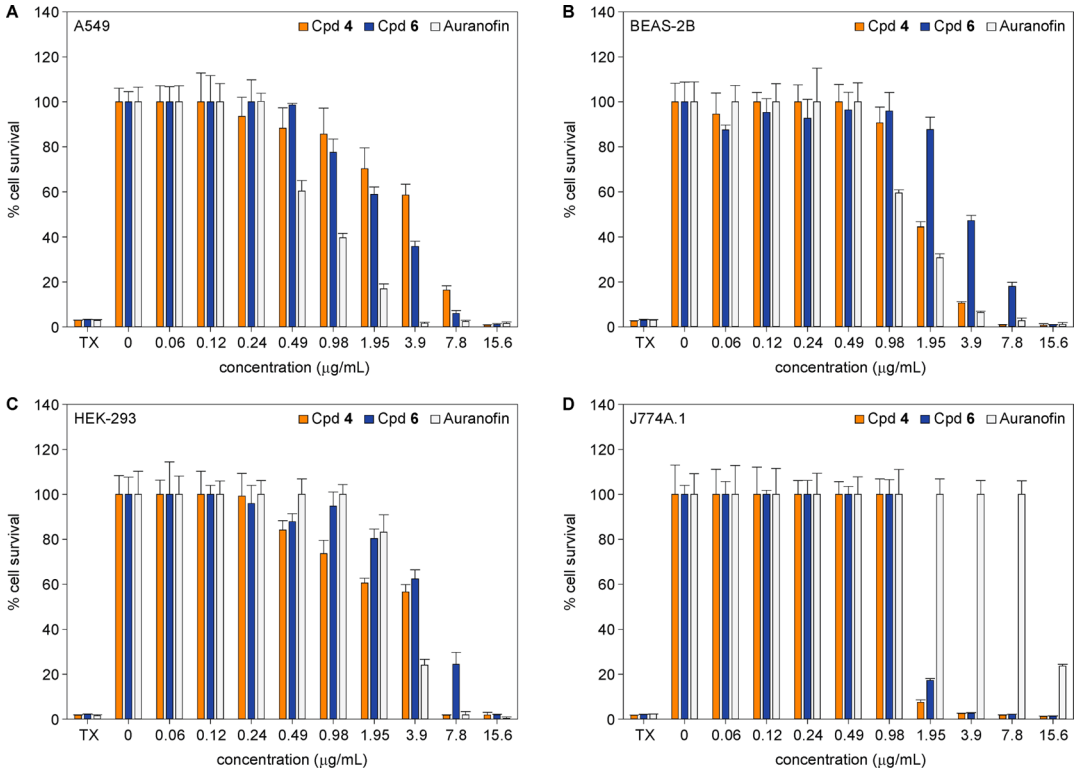

Figure 4. Evaluation of cytotoxicity for compound **4** (orange), compound **6** (blue), and auranofin (white) with (A) A549, (B) BEAS-2B, (C) HEK-293, and (D) J774A.1 cell lines. Controls include treatment with Triton-X (TX, 1% v/v, positive control) and 0.5% DMSO (negative control). Values of >100% were normalized to 100%.

1.95 μg/mL, which are concentrations at which there is toxicity observed for the mammalian cells. Overall, compounds **4** and **6** displayed somewhat better selectivity to kill fungi over mammalian cells than the FDA approved drug, auranofin. Despite this result, there is room to improve these gold complexes to increase the therapeutic window by reducing mammalian cell toxicity.

Reports have suggested that gold complexes bind to thioredoxin reductase in bacteria and mammalian cells,[29,30] but there is some evidence to suggest that gold complexes could inhibit mitochondrial function in fungi.[26] Future studies for the gold complexes, out of scope for this proof-of-concept work, should seek to answer whether these square-planar gold complexes bind thioredoxin reductase or mitochondrial enzymes, which if so, could lead to more in depth structure−activity studies to decrease cytotoxicity. For other reported gold complexes that were investigated for anticancer activity, IC_{50} values for complexes comprising (1*R*,2*R*)-(+)-1,2-diaminocyclohexane ligands ranged from 1.2 to 14.8 μM against cancer cell lines and were >100 μM against a human normal lung fibroblast cell line, MRC5.[42] Another square-planar gold(I) diphosphine complex displayed IC_{50} values of 0.3−9.2 μM.[65] In this report, IC_{50} values ranged from 0.55 to 0.83 μM against two cancer cell lines for both compounds **4** and **6**. Interestingly, an achiral version of these complexes was reported to be insoluble. Furthermore, in a preliminary study with a xenograft model, compounds **4** and **6** were tolerated in mice at a dose of 2 mg/kg (100% survival) or 8 mg/kg (83% and 67% survival, respectively), which suggests an acceptable level of toxicity at lower doses.

Measurement of Hemolysis for Compounds 4 and 6. To expand upon the cytotoxicity results, we obtained both murine and human red blood cells (RBCs) to evaluate the hemolytic activity of compounds **4** and **6** as compared to both auranofin and AmB, as well as to the detergent, Triton-X (positive control) (Figure 5). Some drugs, especially those containing both hydrophobic and hydrophilic components, can disrupt cell membranes to cause hemolysis.[66] Examples of drugs that are known to be hemolytic include AmB as well as cisplatin. With AmB, to minimize hemolytic activity a lipid formulation has been developed.[67] The results are similar for both murine and human RBCs; however, the murine RBCs appear more prone to hemolysis as compounds **4** and **6** displayed 13% and 60% hemolysis, respectively, at 3.9 μg/mL and less than 5% with human RBCs. We observed that both compounds **4** and **6** displayed hemolytic activity at 7.8 μg/mL. AmB exhibited somewhat better values with 30−60% hemolysis at 7.8 μg/mL and 100% hemolysis at 15.6 μg/mL. In contrast, auranofin displayed no hemolytic activity at 15.6 μg/mL. With MIC values for compounds **4** and **6** typically in the range of 0.49−1.95 μg/mL for *Candida* spp., there is a 1- to 2-fold therapeutic window, which is not perfect when comparing to the desired 10-fold therapeutic window.

Whole-Cell Uptake Assay for Compounds 4 and 6. To gain some insight into whether compounds **4** and **6** have an intracellular or extracellular target, the uptake of gold into the cell was measured using inductively coupled plasma optical emission spectroscopy (ICP-OES, Figure 6). Uptake was measured with 100 million yeast cells (Note: this is 2−3× more cells than in MIC and time-kill studies) after 30 min treatment with 10 μM (~5× MIC for compounds **4** and **6** against strain *B* and *H*, respectively; ~10× MIC for compounds **4** and **6** against strain *H* and *B*, respectively) compound. These conditions were chosen to have a significant

DOI: 10.1021/acs.jmedchem.9b01436
J. Med. Chem. 2020, 63, 2455−2469

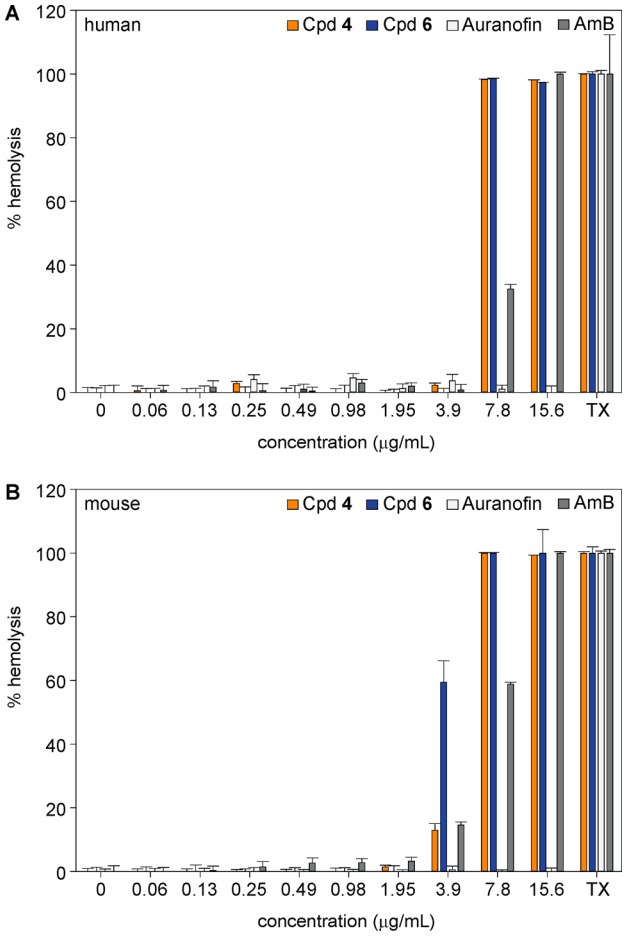

Figure 5. Hemolytic activity of compound **4** (orange), compound **6** (blue), auranofin (white), and AmB (gray) against (A) human and (B) murine red blood cells. Positive control is Triton-X (TX, 1% v/v).

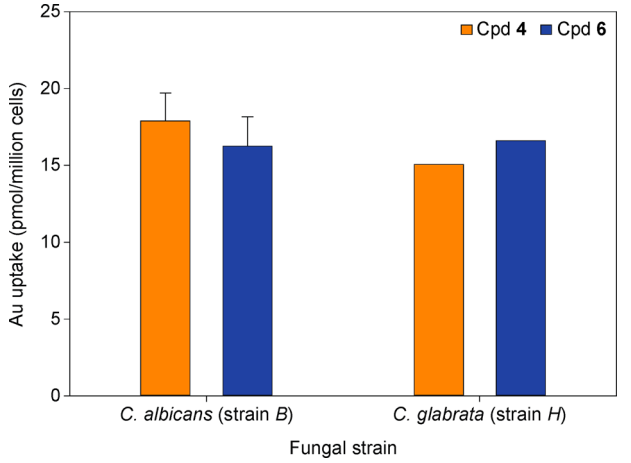

Figure 6. Whole-cell uptake of 10 μM compound **4** (orange) and compound **6** (blue) by *C. albicans* ATCC 10231 (strain *B*) and *C. glabrata* ATCC 2001 (strain *H*) after 30 min treatment.

number of cells for analysis, a saturating amount of compound (note that 10 μM was required to achieve saturation) and at a time-point within the doubling time of the yeast. Both compounds exhibited very similar uptake by *C. albicans* (strain *B*) and *C. glabrata* (strain *H*) of ∼17 pmol/million cells. However, the uptake when 5× MIC was used was higher than when 10× MIC was used. With the values for gold uptake in the pmol/million cells range, there appears to be a relatively low amount of gold uptake per cell, but there are no reports of similar uptake studies in yeast to compare to. However, we do observe uptake and these values correspond to approximately 15% and 20% of total gold content for compounds **4** and **6**, respectively. It is possible that by the 30 min endpoint there is some lysis of the fungal cells, especially with 10× MIC, which would decrease uptake values. These results do suggest that the compounds enter the yeast cell by facilitated diffusion or active transport as with passive diffusion higher dosing of compound (e.g., saturating amount) corresponds to greater cell uptake. We previously published gold(III) complexes that we investigated as anticancer agents, where we measured gold uptake in OVCAR8 cells.[42] We found that gold(III) complexes that included a single chloride anion had improved uptake over similar complexes with perchlorate anions, with relative uptake of ∼300−400 and ∼200 pmol/million cells, respectively. These values were significantly lower than the ∼1300 pmol/million cells uptake of auranofin in the OVCAR8 cell. The uptake values for compounds **4** and **6** in fungi appear significantly lower than the values measured for other complexes with the mammalian cells but are similar when the difference in cell volume and incubation time between yeast and mammalian cells is considered.[68,69] Therefore, it is still unclear but within reason for the gold complexes to have an intracellular target. Conceivably, the structurally complex cell wall of fungus composed of chitin, glucans, and glycoproteins may contribute to the limited uptake of the cationic gold complexes investigated. Further studies will focus on developing neutral complexes and complexes that benefit from active transport.

Development of Fungal Resistance for Compounds 4 and 6. Fungal drug resistance can be caused by mutation of the target protein (observed with azoles and echinocandins),[70,71] overexpression of the target protein (observed with azoles),[72,73] the use of efflux pumps (observed with azoles),[74−78] or increased filamentation to decrease drug uptake (observed with AmB).[79,80] In order to assess the potential for the development of fungal resistance, we determined MIC values of compounds **4** and **6** as well as AmB as a control over 15 serial passages with *C. albicans* (strain *B*) and *C. glabrata* (strain *H*) (Figure S34). We observed no significant changes in MIC values for our compounds over the course of this study. The gold complexes are likely to display different mechanisms of action in fungi that can circumvent resistance pathways.

CONCLUSIONS

In summary, we synthesized three linear gold(I) phosphine complexes and three corresponding square-planar gold(I) complexes and explored their antifungal activity. Two square-planar complexes, **4** and **6**, displayed excellent antifungal activity against a panel of 21 *Candida* strains which included *C. albicans*, *C. glabrata*, *C. krusei*, *C. parapsilosis*, and *C. auris* as well as four *C. neoformans*. Furthermore, these square-planar complexes displayed good activity against four filamentous strains of *Aspergillus* spp. and *Fusarium* spp. In addition, compounds **4** and **6** displayed good activity against *Candida* spp. biofilms. When tested against mammalian cells, the gold complexes displayed limited improvement in selectivity index over the FDA-approved drugs AmB and auranofin. Finally, by development of resistance studies of compounds **4** and **6** in *Candida* spp., it was found that *Candida* spp. has a low chance

DOI: 10.1021/acs.jmedchem.9b01436
J. Med. Chem. 2020, 63, 2455−2469

of developing resistance to these gold complexes. Future studies will work to decrease the toxic effect to mammalian cells and to substantiate the mechanism of action of the gold complexes in fungi.

EXPERIMENTAL SECTION

Chemistry. Materials and Instrumentation. Tetrahydrothiophene (THT) was from Sigma-Aldrich and used without further purification or drying. Tetrachloroauric acid ($HAuCl_4 \bullet 3H_2O$) was purchased from Oakwood and used as received. THT and $HAuCl_4 \bullet 3H_2O$ were used to prepare AuCl(THT) as previously reported.[44] All phosphorus ligands used, 1,2-bis(diphenylphosphino)-benzene, 1,2-bis[(2*S*,5*S*)-2,5-dimethylphospholano]benzene, and 1,2-bis[(2*R*,5*R*)-2,5-dimethylphospholano]benzene, were purchased from Sigma-Aldrich and used as received. ACS grade solvents were purchased from Pharmco-Aaper and used without further purification or drying. Deuterated solvents were purchased from Cambridge Isotope Laboratories and used as received. Silica gel for column chromatography (Silicycle, P/N R10030B SiliaFlashF60, size 40−63 μm, Canada) was purchased from Silicycle. Aluminum backed silica-gel plates (20 × 20 cm^2) were purchased from Silicycle (TLA-R10011B-323) and utilized for analytical thin-layer chromatography (TLC).

All reactions were insensitive to air or moisture; as a result, they were carried out under standard atmospheric conditions without air-sensitive techniques or drying agents. Reactions were carried out in round-bottom flasks or scintillation vials equipped with Teflon-coated magnetic stir bars for stirring nonhomogenous reaction mixtures. Reactions were monitored by NMR and TLC, and the TLC plates were visualized under short-wavelength light (254 nm) or stained with iodine on silica. All compound purification was performed using silica-gel chromatography, employing CombiFlash Rf+ Lumen, Teledyne ISCO. Filtrations were carried out using medium-porosity ceramic funnels. Removal of solvents in vacuo was performed using a Büchi rotary evaporator, and further drying was achieved by Schlenk line at ∼120 mTorr using a dynamic vacuum pump.

^1H, ^{13}C (^1H-decoupled), and ^{31}P (^1H-decoupled) NMR spectra were recorded on a Varian Unity 400 MHz NMR spectrometer with a Spectro Spin superconducting magnet at the University of Kentucky NMR facility in the Department of Chemistry. Chemical shifts in ^1H and ^{13}C NMR spectra were internally referenced to solvent signals (^1H NMR, $CDCl_3$ at δ = 7.26 ppm; ^{13}C NMR, $CDCl_3$ at δ = 77.16 ppm), and those in ^{31}P NMR spectra, which were run in $CDCl_3$, were externally referenced to 85% H_3PO_4 in D_2O at δ = 0 ppm.

High-resolution mass spectra (HRMS) were obtained using a direct flow injection (injection volume = 1 μL) method with electrospray ionization (ESI) on a Waters Q-TOF Premier instrument in the positive mode. The optimized conditions were as follows: capillary = 3000 kV, cone = 35, source temperature = 120 °C, and desolvation temperature = 350 °C. Mass spectrometry experiments and analysis were conducted at the Chemical Instrumentation Center at Boston University.

In addition to spectroscopic characterization, the purity of all compounds was assessed by RP-HPLC using an Agilent Technologies 1100 series HPLC instrument and an Agilent Phase Eclipse Plus C18 column (4.6 mm × 100 mm; 3.5 μm particle size). All compounds were found to be ≥97% pure.

Synthesis and Characterization of Compounds 1−6. Synthesis of the Known Compounds [1,2-Bis-(diphenylphosphino)benzene]digold(I) (1)[45] and Bis-[1,2-bis-(diphenylphosphino)benzene]gold(I) (2).[46] Under normal atmospheric conditions, in a 25 mL round-bottom flask was placed AuCl(THT) (58.7 mg, 0.183 mmol). $CHCl_3$ (10.0 mL) was added, and the solution (white suspension) was stirred at room temperature for 2−3 min. To the solution was added 1,2-bis(diphenylphosphino)-benzene (80.2 mg, 0.180 mmol). The solution turned yellow instantly. The solution was stirred for about 1 h and monitored by TLC using 5:95 MeOH:CH_2Cl_2 as an eluent. Separation of compounds **1** and **2** was achieved via flash chromatography using CombiFlash Rf+ Lumen with 5:95 MeOH:CH_2Cl_2.

Characterization of Compound ***1***. White solid (37 mg, 23%); R_f = 0.8 in 5:95 MeOH:CH_2Cl_2; ^1H NMR (400 MHz, $CDCl_3$, Figure S1) δ 7.56−7.46 (m, 6H), 7.46−7.35 (m, 16H), 7.25−7.16 (m, 2H); ^{13}C NMR (101 MHz, $CDCl_3$, Figure S2) δ 137.12, 137.05, 136.97, 134.81, 134.74, 134.67, 132.35, 131.90, 131.87, 131.84, 129.60, 129.54, 129.48, 128.91, 128.60, 128.28; ^{31}P NMR (162 MHz, $CDCl_3$, Figure S3) δ 24.60. HRMS (ESI) (m/z): calcd for $C_{30}H_{24}Au_2Cl_2P_2$ $[M - Cl]^+$, 875.0373; found, 875.0408 Δ = 3.9998 (Figure S4). Purity was demonstrated to be 97% by RP-HPLC: t_R = 8.82 min using the following method. Flow rate: 1 mL/min; λ = 260 nm; eluent A = H_2O with 0.1% TFA; eluent B = MeCN with 0.05% formic acid. Elution program: 0 to 100% B over 10 min followed by 100 to 0% B over 5 min and 4 additional min at 0% B (Figure S5).

Characterization of Compound ***2***. Yellow solid (68 mg, 36%); R_f = 0.2 in 5:95 MeOH:CH_2Cl_2; ^1H NMR (400 MHz, $CDCl_3$, Figure S6) δ 7.57−7.25 (m, 20H), 7.13−6.87 (m, 28H); ^{13}C NMR (101 MHz, $CDCl_3$, Figure S7) δ 142.13, 134.52, 134.37, 132.56, 132.44, 132.37, 132.33, 132.29, 132.25, 132.21, 132.18, 131.72, 130.40, 129.13, 129.11, 129.08, 129.06, 129.03, 129.01, 128.89, 128.86, 128.74; ^{31}P NMR (162 MHz, $CDCl_3$, Figure S8) δ 21.17. HRMS (ESI) (m/z): calcd for $C_{60}H_{48}AuClP_4$ $[M - Cl]^+$, 1089.2372; found, 1089.2357 Δ = 1.3771 (Figure S9). Purity was demonstrated to be 100% by RP-HPLC: t_R = 10.78 min using the following method. Flow rate: 1 mL/min; λ = 260 nm; eluent A = H_2O with 0.1% TFA; eluent B = MeOH with 0.1% TFA. Elution program: 0 to 100% B over 5 min, stay at 100% B for 10 min, followed by 100 to 0% B over 4 min (Figure S10).

Synthesis of [1,2-Bis[(2*S*,5*S*)-2,5-dimethylphospholano]-benzene]digold(I) (3) and Bis-[1,2-bis[(2*S*,5*S*)-2,5-dimethylphospholano]benzene]gold(I) (4). Compounds **3** and **4** were synthesized and separated following the procedure described for the preparation of compounds **1** and **2** using AuCl(THT) (64.6 mg, 0.202 mmol) and 1,2-bis[(2*S*,5*S*)-2,5-dimethyl-1-phospholano]-benzene (58.6 mg, 0.191 mmol).

Characterization of Compound ***3***. White solid (47 mg, 32%); R_f = 0.8 in 5:95 MeOH:CH_2Cl_2; ^1H NMR (400 MHz, $CDCl_3$, Figure S11) δ 7.73−7.64 (m, 4H), 3.60 (sextet, J = 7.6 Hz, 2H), 2.99−2.85 (m, 2H), 2.53−2.38 (m, 2H), 2.30−2.13 (m, 2H), 1.92−1.77 (m, 2H), 1.57−1.44 (m, 2H), 1.37 (dd, J = 20.6, 6.7 Hz, 6H), 1.06 (dd, J = 17.2, 7.2 Hz, 6H); ^{13}C NMR (101 MHz, $CDCl_3$, Figure S12) δ 134.45, 134.39, 134.33, 132.19, 131.61, 131.58, 131.56, 37.20, 37.03, 37.01, 36.97, 36.84, 36.79, 36.61, 35.56, 35.54, 33.99, 33.92, 33.85, 19.59, 19.56, 19.52, 19.47, 19.42; ^{31}P NMR (162 MHz, $CDCl_3$, Figure S13) δ 43.96. HRMS (ESI) (m/z): calcd for $C_{18}H_{28}Au_2Cl_2P_2$ $[M - Cl]^+$, 735.0686; found, 735.0671 Δ = 2.0406 (Figure S14). Purity was demonstrated to be 97% by RP-HPLC: t_R = 7.94 min using the following method. Flow rate: 1 mL/min; λ = 260 nm; eluent A = H_2O with 0.1% TFA; eluent B = MeCN with 0.05% formic acid. Elution program: 0 to 100% B over 10 min followed by 100 to 0% B over 5 min and 4 additional min at 0% B (Figure S15).

Characterization of Compound ***4***. Yellow solid (44 mg, 27%); R_f = 0.4 in 5:95 MeOH:CH_2Cl_2; ^1H NMR (400 MHz, $CDCl_3$, Figure S16) δ 7.75−7.67 (m, 4H), 7.60−7.54 (m, 4H), 2.71−2.46 (m, 8H), 2.35−2.13 (m, 8H), 1.87−1.72 (m, 4H), 1.62−1.49 (m, 4H), 1.19 (td, J = 10.6, 6.9 Hz, 12H), 0.81−0.71 (m, 12H); ^{13}C NMR (101 MHz, $CDCl_3$, Figure S17) δ 142.52, 142.36, 142.20, 133.34, 133.31, 133.29, 130.67, 40.56, 40.48, 40.40, 37.71, 37.65, 37.59, 36.06, 35.84, 21.47, 21.41, 21.36, 14.49; ^{31}P NMR (162 MHz, $CDCl_3$, Figure S18) δ 38.34. HRMS (ESI) (m/z): calcd for $C_{36}H_{56}AuClP_4$ $[M - Cl]^+$, 809.2998; found, 809.3016 Δ = 2.2241 (Figure S19). Purity was demonstrated to be 98% by RP-HPLC: t_R = 10.81 min using the following method. Flow rate: 1 mL/min; λ = 260 nm; eluent A = H_2O with 0.1% TFA; eluent B = MeCN with 0.05% formic acid. Elution program: 0 to 100% B over 10 min followed by 100 to 0% B over 5 min and 4 additional min at 0% B (Figure S20).

Synthesis of the Known Compounds [1,2-Bis[(2*R*,5*R*)-2,5-dimethylphospholano]benzene]digold(I) (5)[81] and Bis-[1,2-bis[(2*R*,5*R*)-2,5-dimethylphospholano]benzene]gold(I) (6).

DOI: 10.1021/acs.jmedchem.9b01436
J. Med. Chem. 2020, 63, 2455−2469

Compounds **5** and **6** were synthesized and separated following the procedure described for the preparation of compounds **1** and **2** using AuCl(THT) (61.9 mg, 0.193 mmol) and 1,2-bis[(2*R*,5*R*)-2,5-dimethylphospholano]benzene (60.1 mg, 0.196 mmol).

Characterization of Compound ***5***. White powder (35 mg, 35%); R_f = 0.8 in 5:95 MeOH:CH_2Cl_2; ^{1}H NMR (400 MHz, $CDCl_3$, Figure S21) δ 7.73−7.64 (m, 4H), 3.61 (sextet, J = 7.7 Hz, 2H), 2.99−2.86 (m, 2H), 2.54−2.38 (m, 2H), 2.30−2.12 (m, 2H), 1.92−1.76 (m, 2H), 1.56−1.44 (m, 2H), 1.37 (dd, J = 20.6, 6.8 Hz, 6H), 1.06 (dd, J = 17.2, 7.2 Hz, 6H); ^{13}C NMR (101 MHz, $CDCl_3$, Figure S22) δ 134.62, 134.56, 134.49, 131.75, 131.72, 131.70, 37.37, 37.20, 37.19, 37.16, 37.02, 36.99, 36.81, 35.73, 35.71, 35.69, 34.17, 34.10, 34.03, 19.73, 19.71, 19.68, 19.63, 19.57; ^{31}P NMR (162 MHz, $CDCl_3$, Figure S23) δ 43.96. HRMS (ESI) (m/z): calcd for $C_{18}H_{28}Au_2Cl_2P_2$ [M − Cl]$^+$, 735.0686; found, 735.0697 Δ = 1.4965 (Figure S24). Purity was demonstrated to be 97% by RP-HPLC: t_R = 7.86 min using the following method. Flow rate: 1 mL/min; λ = 260 nm; eluent A = H_2O with 0.1% TFA; eluent B = MeCN with 0.05% formic acid. Elution program: 0 to 100% B over 10 min followed by 100 to 0% B over 5 min and 4 additional min at 0% B (Figure S25).

Characterization of Compound ***6***. Yellow powder (71 mg, 37%); R_f = 0.2 in 5:95 MeOH:CH_2Cl_2; ^{1}H NMR (400 MHz, $CDCl_3$, Figure S26) δ 7.74−7.66 (m, 4H), 7.60−7.53 (m, 4H), 2.71−2.44 (m, 8H), 2.35−2.13 (m, 8H), 1.86−1.72 (m, 4H), 1.61−1.48 (m, 4H), 1.18 (td, J = 10.5, 6.8 Hz, 12H), 0.80−0.71 (m, 12H); ^{13}C NMR (101 MHz, $CDCl_3$, Figure S27) δ 142.34, 133.32, 133.29, 133.27, 130.66, 40.54, 40.46, 40.39, 37.69, 37.63, 37.56, 36.04, 35.82, 21.45, 21.39, 21.34, 14.47; ^{31}P NMR (162 MHz, $CDCl_3$, Figure S28) δ 38.24. HRMS (ESI) (m/z): calcd for $C_{36}H_{56}AuClP_4$ [M − Cl]$^+$, 809.2998; found, 809.3025 Δ = 3.3362 (Figure S29). Purity was demonstrated to be 97% by RP-HPLC: t_R = 10.81 min using the following method. Flow rate: 1 mL/min; λ = 260 nm; eluent A = H_2O with 0.1% TFA; eluent B = MeCN with 0.05% formic acid. Elution program: 0 to 100% B over 10 min followed by 100 to 0% B over 5 min and 4 additional min at 0% B (Figure S30).

X-ray Crystallography of Compounds 3−6. The single crystal of compound **3** was grown at 4 °C by vapor diffusion of Et_2O into a CH_2Cl_2 solution, and compounds **4**, **5**, and **6** were grown at room temperature by vapor diffusion of Et_2O into $CDCl_3$ solutions. Suitable crystals were selected by microscopic examination through crossed polarizers, mounted on a fine glass fiber in polyisobutene oil, and cooled to 90 K under a stream of nitrogen. A Bruker D8 Venture diffractometer with graded-multilayer focused MoKα X-rays (λ = 0.710 73 Å) was used to collect the diffraction data from the crystals. The raw data were integrated, scaled, merged, and corrected for Lorentz polarization effects using the APEX3 package.[82,83] Space group determination and structure solution and refinement were carried out with SHELXT and SHELXL,[84,85] respectively. All non-hydrogen atoms were refined with anisotropic displacement parameters. Hydrogen atoms were placed at calculated positions and refined using a riding model with their isotropic displacement parameters (U_{iso}) set to either 1.2U_{iso} or 1.5U_{iso} of the atom to which they were attached. The structures, deposited in the Cambridge Structural Database (deposition number = 1889869 (**3**), 1889576 (**4**), 1889577 (**5**), and 1916580 (**6**)), were checked for missed higher symmetry, twinning, and overall quality with PLATON,[86] an **R**-tensor,[87] and finally validated using CheckCIF.[86] The X-ray structures of compounds **3**−**6** are presented in Figure 2 and the corresponding structure refinement data in Table S1.

Biochemistry and Microbiology. Biochemical/Biological Reagents and Instrumentation. The American Type Culture Collection (ATCC) *Candida albicans* strains, including 10231 (strain *B*), MYA-2876 (strain *E*), and 64124 (strain *F*), were a generous gift from Dr. Jon Y. Takemoto (Utah State University, Logan, UT, USA). The rest of the *C. albicans* strains, including MYA-1003 (strain *A*), MYA-1237 (strain *C*), MYA-2310 (strain *D*), 90819 (strain *G*), and the non-*albicans Candida* fungi *C. glabrata* ATCC 2001 (strain *H*), *C. krusei* ATCC 6258 (strain *I*), *C. parapsilosis* ATCC 22019 (strain *J*), and *Cryptococcus neoformans* ATCC MYA-85 (strain *M*) were purchased from the American Type Culture Collection (ATCC, Manassas, VA, USA). A panel of *Candida auris* strains were acquired from the CDC & FDA Antibiotic Resistance Isolate Bank (CDC, Atlanta, GA, USA), which included *C. auris* AR bank no. 0381-0390 (strains *K*, *L*, and I−VIII). *C. neoformans* clinical isolates CN1-CN3 (strains *N*−*P*) were generously provided by Dr. Nathan Wiederhold (University of Texas, San Antonio, TX, USA). The filamentous fungi *Aspergillus nidulans* ATCC 38163 (strain *Q*) and *Fusarium graminearum* 053 (strain *T*) were kind gifts from Prof. Jon S. Thorson (University of Kentucky, Lexington, KY) and Prof. Lisa Vaillancourt (University of Kentucky, Lexington, KY, USA), while the *Aspergillus terreus* ATCC MYA-3633 (strain *R*) and *Aspergillus flavus* ATCC MYA-3631 (strain *S*) were purchased from the ATCC. Yeast strains were cultured at 35 °C in yeast extract peptone dextrose (YEPD) broth. *Aspergillus* spp. strains were cultured on potato dextrose agar (PDA, catalog no. 110130, EMD Millipore, Billerica, MA, USA) at 28 °C before the spores were harvested. All fungal experiments were carried out in RPMI 1640 medium (catalog no. R6504, Sigma-Aldrich, St. Louis, MO, USA) buffered to pH 7.0 with 0.165 M MOPS buffer (Sigma-Aldrich, St. Louis, MO, USA).

For cytotoxicity assays, the human embryonic kidney cell line (HEK-293) was purchased from the ATCC. The human bronchial epithelial cell line (BEAS-2B), the human lung carcinoma cell line (A549), and the mouse macrophage cell line (J774A.1) were generous gifts from Prof. David K. Orren (University of Kentucky, Lexington, KY), Prof. Markos Leggas (University of Kentucky, Lexington, KY), and Prof. David J. Feola (University of Kentucky, Lexington, KY), respectively. A549, HEK-293, and BEAS-2B cells were cultured in Dulbecco's modified Eagle's medium (DMEM, catalog no. VWRL0100, VWR, Chicago, IL) supplemented with 10% fetal bovine serum (FBS; from ATCC) and 1% penicillin/streptomycin (from ATCC) at 37 °C with 5% CO_2. The J774A.1 cells were cultured in DMEM (catalog no. 30-2002, ATCC, Manassas, VA), which was also supplemented with FBS and antibiotics and grown at 37 °C with 5% CO_2.

Instruments for fungal assays with yeast were the V-1200 spectrophotometer (VWR, Radnor, PA, USA) and the SpectraMax M5 plate reader (Molecular Devices, Sunnyvale, CA, USA) for biofilm, cytotoxicity, and hemolysis assays. For the whole-cell uptake assay, an inductively coupled plasma optical emission spectroscopy instrument was used (ICP-OES, Agilent, Santa Clara, CA, USA). The known antifungal drugs, amphotericin B (AmB, VWR, Chicago, IL, USA), caspofungin (CAS, Sigma-Aldrich, St. Louis, MO, USA), fluconazole (FLC, AK Scientific, Union City, CA, USA), voriconazole (VRC, AK Scientific, Union City, CA, USA), and the antirheumatic drug, auranofin (Santa Cruz Biotechnology, Dallas, TX, USA) were used as positive controls.

Determination of Minimum Inhibitory Concentration (MIC) Values of Compounds 1−6. The individual minimum inhibitory concentration (MIC) values of compounds **1**−**6** were measured for each fungal strain. The MIC values were determined using the broth microdilution method[88] in sterile 96-well plates. Concentrations of compound tested were 0.06−31.3 μg/mL. For testing, compounds were dissolved in DMSO at a concentration of 5 mg/mL allowing the highest concentration of DMSO to be 0.63% in the assay. Serial 2-fold dilutions of compound were made horizontally across the plate in 100 μL of RPMI 1640 medium. For yeast, the overnight culture was diluted into RPMI 1640 (25 μL of a fungal stock with OD_{600} of 0.12−0.15 into 10 mL of RPMI 1640 medium, resulting in final inoculum size around (1−5) × 10^3 CFU/mL) and added to the plate (100 μL per well), making a final volume of 200 μL total per well. Similarly, for *Aspergillus* spp. and *F. graminearum* 053, spores were diluted in RPMI 1640 to 5 × 10^5 spores/mL and then 100 μL of stock was seeded in each well.[89] The MIC-0 value of each compound was determined by visual inspection, and MIC-2 values were measured via optical density reading at 600 nm. For *Candida* spp., plates were incubated for 48 h at 35 °C. For *Cryptococcus* spp. and *Aspergillus* spp. plates were incubated for 72 h at 35 °C, and *F. graminearum* 053 the plate was incubated at room temperature for 5 days. MIC values for CAS were read at 24 h (Tables 1 and 2).

DOI: 10.1021/acs.jmedchem.9b01436
J. Med. Chem. 2020, 63, 2455−2469

Time−Kill Assays for Compounds 4 and 6. To assess the time-dependent inhibition of compounds **4** and **6** against four yeast strains, *C. albicans* ATCC 10231 (strain *B*), *C. glabrata* ATCC 2001 (strain *H*), *C. auris* AR bank no. 0384 (strain *K*), and *C. auris* AR bank no. 0390 (strain *L*), we performed time−kill assays. The protocol for time−kill assays followed methods previously described with minor modifications.[34,90] Overnight cultures were grown in YEPD medium at 35 °C with shaking at 200 rpm. The overnight cultures were diluted in RPMI 1640 medium to an OD_{600} of 0.125 (~1×10^6 CFU/mL). Then, an amount of 200 μL of cells was added to 4.8 mL of RPMI 1640 medium in sterile culture tubes to afford a fungal cell concentration of ~1×10^5 CFU/mL. Compounds were then added to the fungal cells. The treatment conditions included sterile control (negative control), growth control, compound **4** at 1× MIC, **4** at 2× MIC, **6** at 1× MIC, **6** at 2× MIC, as well as AmB at 1× MIC as a positive control. Treated fungal cultures were incubated in the culture tubes at 35 °C with 200 rpm shaking for 24 h. Samples were aliquoted from the different treatments at regular time points (0, 3, 6, 9, 12, and 24 h) and plated in duplicate onto PDA plates. For each time point, cultures were vortexed, 100 μL of culture was aspirated, and 10-fold serial dilutions were made in sterile ddH_2O. From the appropriate dilutions, 100 μL of fungal suspension was spread on agar plates and incubated at 35 °C for 48 h before colony counts were determined. Only plates containing between 30 and 300 colonies were counted, making 30 CFU/mL the limit of detection. At 24 h, 50 μL of sterile 2 mM resazurin in phosphate buffered saline (PBS) was added to the treatments and incubated at 35 °C with 200 rpm shaking for 2 h in the dark for visual inspection. As resazurin (blue-purple) is metabolized by the cells to produce resorufin (pink-orange), the addition of resazurin is used as a qualitative measure to confirm the relative growth of the fungal cells in the different treatment conditions (Figure 3).

Prevention of Biofilm Formation and Disruption of Preformed Biofilm Assays for Compounds 4 and 6. To evaluate the ability of the gold complexes to prevent formation of biofilms and also their ability to disrupt preformed biofilms, we conducted assays for compounds **4** and **6** against sessile yeast cells for four representative yeast strains, *C. albicans* ATCC 10231 (strain *B*), *C. glabrata* ATCC 2001 (strain *H*), *C. auris* AR bank no. 0384 (strain *K*), and *C. auris* AR bank no. 0390 (strain *L*). All biofilm assays were performed in 96-well plates using XTT [2,3-bis(2-methoxy-4-nitro-5-sulfophenyl)-2*H*-tetrazolium-5-carboxanilide] to measure the viability of the biofilm as previously described.[91,92] An overnight culture of yeast was grown at 35 °C in YEPD medium with shaking at 200 rpm before dilution in RPMI 1640 medium to an OD_{600} between 0.12 and 0.15. For biofilm prevention assays, serial dilutions of compounds were made in 100 μL of RPMI as in the MIC assays and 100 μL of fungal suspension with OD_{600} of 0.12−0.15 was added. For assays with a preformed biofilm, 100 μL of fungal cells were aliquoted in a 96-well plate, leaving one column empty for the sterile control. After 24 h incubation at 37 °C, visible biofilms had formed in the well. The biofilm was washed three times with 100 μL of PBS. After washing, RPMI 1640 medium and compound were added to the plate, in a similar fashion to that described for the MIC values. All compounds were tested in the concentration range of 0.06−31.3 μg/mL, and AmB and auranofin were included as controls. Plates were incubated at 37 °C for 24 h. Finally, the plates were washed three times with PBS before adding 100 μL of XTT dye. The XTT was prepared by dissolving XTT at 0.5 mg/mL concentration in sterile PBS. Before addition to a plate, 1 μL of 10 mM menadione in acetone was added to 10 mL of the 0.5 mg/mL solution of XTT. After addition of XTT (containing menadione), the plates were incubated for 3 h at 37 °C in the dark. 80 μL of liquid from each well was transferred to a new plate and then with the plate reader for absorbance at 450 nm. For these experiments, we determined the sessile MIC ($SMIC_{90}$), which is defined as the compound concentration required to inhibit the metabolic activity of biofilm by 90% compared to the growth control (Table 3). The plates used to determine the $SMIC_{90}$ values are provided in Figure S31 (prevention of biofilm formation) and Figure S32 (disruption of preformed biofilm). Each assay was performed in duplicate.

Mammalian Cytotoxicity Assays for Compounds 4 and 6. To examine whether the compounds are safe for human cells, cytotoxicity assays were done against four mammalian cell lines: HEK-293, A549, BEAS-2B, and J774A.1 cells. Compounds **4** and **6** as well as auranofin were tested against each cell line to measure their cytotoxic effect by using a resazurin cell viability assay as previously described with minor modifications.[35,93] The assays were done in 96-well plates, and cell counts were made using a hemacytometer. HEK-293 and J774A.1 cells were plated at 1×10^4 cells/mL, while A549 and BEAS-2B were plated at 3×10^3 cells/mL. Compounds were tested in concentrations ranging from 0.06 to 15.6 μg/mL with final concentration of DMSO at 0.5% (Figure 4). It is important to note that testing xenobiotics at sub-IC_{50} concentrations can result in increase in cell growth, resulting in >100% cell survival in the treatment groups.[94−98] In instances where >100% cell survival was observed, we displayed the data as 100% cell survival in Figure 4. We are providing the data with observed % in Figure S33. All assays were done in quadruplicate.

Measurement of Hemolysis for Compounds 4 and 6. To extend on the cytotoxicity results, compounds **4** and **6** along with auranofin and AmB were tested for their ability to lyse red blood cells (RBCs). Both human and murine RBCs were provided in a citrate-treated tube on ice, and the hemolysis assay was done as previously described with minor modifications and in similar fashion to cytotoxicity assays.[39,99,100] The RBCs were washed three times in PBS by resuspending 0.5 mL of RBCs in 5 mL of PBS and pelleting at 1000 rpm for 7 min. The RBCs were resuspended in PBS to achieve a cell concentration on the order of 10^7 cells/mL. Compounds were dissolved at concentration of 3.14 mg/mL (200×) in DMSO. Serial double dilutions were made in DMSO. A 1:100 dilution of compound in PBS was added to 100 μL of RBCs in a 96-well plate (total volume of 200 μL). Compounds were tested in the range of 0.06−15.6 μg/mL in quadruplicate with 0.5% DMSO and ~5×10^6 RBCs per tube. The RBCs were also treated with 1% Triton-X (positive control) and PBS (negative control). The RBCs were treated for 30 min at 37 °C, and the absorbance was read at 595 nm. Hemolysis is visually observed by a decrease in optical density of the wells (turbid, dark red to transparent pink). Percent hemolysis (Figure 5) was calculated using this equation after subtraction of the background absorbance (positive control):

$$\%\ \text{hemolysis} = \frac{\text{absorbance of sample}}{\text{absorbance of RBC} + \text{PBS (negative control)}} \times 100$$

Whole-Cell Uptake Assay for Compounds 4 and 6. To gain insight into the mechanism of action of these compounds, we measured the uptake of the gold-containing compounds into the yeast cells. Compounds **4** and **6** were each tested with *C. albicans* ATCC 10231 (strain *B*) and *C. glabrata* ATCC 2001 (strain *H*) in independent triplicates following protocols for whole-cell uptake assays as previously described with minor modifications.[42,101,102] A single colony was used to inoculate 3 mL of YEPD, which was grown overnight at 35 °C with 200 rpm shaking. Overnight culture was diluted into 100 mL of YEPD to an OD_{600} of ~0.075 and grown at 35 °C with 200 rpm shaking for 4−6 h until the culture reached an OD_{600} of ~0.3 indicating logarithmic phase growth. The cells were pelleted by centrifugation at 500*g* for 5 min at room temperature and diluted in RPMI to 10^8 cells/mL in RPMI 1640 medium as determined by counting with a hemacytometer. 1 mL of fungal suspension was aliquoted into a 12 mL culture tube. Treatment conditions included 10 μM compound, growth control (no compound), medium with compound (no cells), and 10 μM (8.5 μL) compound for ICP-OES analysis (100% signal). Each treatment was tested in duplicate at 35 °C with 200 rpm shaking. After 30 min of treatment, cells were pelleted by centrifugation at 3000 rpm (~1000*g*) for 5 min. Cell pellets were washed twice with 1 mL of ice-cold PBS. Cell pellets were digested in 0.5 mL of concentrated HCl and added to 4.5 mL of ddH_2O (10% final concentration of HCl). Samples were analyzed for gold content using ICP-OES. Data

DOI: 10.1021/acs.jmedchem.9b01436
J. Med. Chem. 2020, 63, 2455−2469

presented (Figure 6) show values for 10 μM compound after subtraction of values for media with compound.

Development of Fungal Resistance for Compounds 4 and 6. To assess the rate at which fungal strains can develop resistance to the gold compounds, fungal cells were repeatedly exposed to subinhibitory amounts of compound and the MIC values for each subculture were monitored. The procedure for the development of resistance assay was modified for fungal cells following the reported method.[99] MIC assays were done as described above for compounds **4**, **6**, and AmB against *C. albicans* ATCC 10231 (strain *B*) and *C. glabrata* ATCC 2001 (strain *H*). Overnight cultures were inoculated from fungal cells exposed to $^1/_2$ the MIC concentration for each compound. This was repeated for 15 subcultures (Figure S34).

■ ASSOCIATED CONTENT

Supporting Information

The Supporting Information is available free of charge at https://pubs.acs.org/doi/10.1021/acs.jmedchem.9b01436.

Crystal data and structure refinement for compounds **3**−**6** (Table S1); ^{1}H, ^{13}C, ^{31}P spectra, HPLC traces, and HRMS spectra for compounds **1**−**6** (Figures S1−S30); images of 96-well plates from biofilm assays (Figures S31 and S32); cytotoxicity graphs displaying raw data before being normalized to 100% (Figure S33), and plot for development of resistance assay (Figure S34) (PDF)

Molecular formula strings (CSV)

■ AUTHOR INFORMATION

Corresponding Authors

*S.G.A.: e-mail, awuah@uky.edu.
*S.G.-T.: e-mail, sylviegtsodikova@uky.edu.

ORCID

Samuel G. Awuah: 0000-0003-4947-7283
Sylvie Garneau-Tsodikova: 0000-0002-7961-5555

Author Contributions

E.K.D. and S.G.-T. designed all the biochemical and biological studies. S.G.A. and J.H.K. designed the synthesis of compounds **1**−**6**. E.K.D. performed all biochemical and biological experiments. J.H.K. synthesized compounds **1**−**6** and characterized the compounds. S.P. solved the X-ray structures of compounds **3**−**6**. E.K.D. and S.G.-T. wrote the manuscript and Supporting Information and made all figures. All authors provided feedback on the manuscript and Supporting Information and have given approval to the final version of the manuscript and Supporting Information.

Notes

The authors declare no competing financial interest.

■ ACKNOWLEDGMENTS

This work was supported in part by a University of Kentucky Igniting Research Collaborations pilot grant, funded by the Vice President for Research and College Deans (to S.G.-T. and S.G.A.), and startup funds from the University of Kentucky (to S.G.-T. and S.G.A.). We also thank the University of Kentucky's Environmental Research Training Laboratory (ERTL) for their assistance with the ICP-OES, Prof. Sidney Whiteheart for providing the red blood cells for the hemolysis studies, and Dr. Norman Lee of the Chemical Instrumentation Center at Boston University for mass spectrometry analysis. Crystallography at the University of Kentucky is supported by NSF MRI Award CHE1625732 (to S.P.).

■ ABBREVIATIONS USED

AmB, amphotericin B; ATCC, American Type Culture Collection; CAS, caspofungin; CFU, colony forming unit; ESI, electrospray ionization; FLC, fluconazole; HRMS, high resolution mass spectrometry; ICP-OES, inductively coupled plasma optical emission spectroscopy; MIC, minimal inhibitory concentration; PBS, phosphate buffered saline; RBC, red blood cell; RP-HPLC, reverse-phase high-performance liquid chromatography; SMIC, sessile minimal inhibitory concentration; THT, tetrahydrothiophene; TLC, thin layer chromatography; VRC, voriconazole

■ REFERENCES

(1) Bongomin, F.; Gago, S.; Oladele, R. O.; Denning, D. W. Global and multi-national prevalence of fungal diseases-estimate precision. *J. Fungi (Basel)* **2017**, *3*, 57.
(2) Brown, G. D.; Denning, D. W.; Gow, N. A.; Levitz, S. M.; Netea, M. G.; White, T. C. Hidden killers: Human fungal infections. *Sci. Transl. Med.* **2012**, *4*, 165rv13.
(3) Lockhart, S. R.; Iqbal, N.; Cleveland, A. A.; Farley, M. M.; Harrison, L. H.; Bolden, C. B.; Baughman, W.; Stein, B.; Hollick, R.; Park, B. J.; Chiller, T. Species identification and antifungal susceptibility testing of *Candida* bloodstream isolates from population-based surveillance studies in two U.S. cities from 2008 to 2011. *J. Clin. Microbiol.* **2012**, *50*, 3435−3442.
(4) Bassetti, M.; Bouza, E. Invasive mould infections in the ICU setting: Complexities and solutions. *J. Antimicrob. Chemother.* **2017**, *72*, i39−i47.
(5) Arendrup, M. C.; Perlin, D. S. Echinocandin resistance: An emerging clinical problem? *Curr. Opin. Infect. Dis.* **2014**, *27*, 484−492.
(6) Jeffery-Smith, A.; Taori, S. K.; Schelenz, S.; Jeffery, K.; Johnson, E. M.; Borman, A.; Candida auris Incident Management Team; Manuel, R.; Brown, C. S. *Candida auris*: A review of the literature. *Clin. Microbiol. Rev.* **2018**, *31*, e00029−17.
(7) Sarma, S.; Upadhyay, S. Current perspective on emergence, diagnosis and drug resistance in *Candida auris*. *Infect. Drug Resist.* **2017**, *10*, 155−165.
(8) Richtel, M. To fight deadly *Candida auris*, New York State proposes new tactics. *N. Y. Times* **2019** (May 23).
(9) Richtel, M. *Candida auris*: The fungus nobody wants to talk about. *N. Y. Times* **2019** (April 8).
(10) Richtel, M.; Jacobs, A. A mysterious infection spanning the globe in a climate of secracy. *N. Y. Times* **2019** (April 6).
(11) Yu, Z.; Gunn, L.; Wall, P.; Fanning, S. Antimicrobial resistance and its association with tolerance to heavy metals in agriculture production. *Food Microbiol.* **2017**, *64*, 23−32.
(12) Lazarevic, T.; Rilak, A.; Bugarcic, Z. D. Platinum, palladium, gold and ruthenium complexes as anticancer agents: Current clinical uses, cytotoxicity studies and future perspectives. *Eur. J. Med. Chem.* **2017**, *142*, 8−31.
(13) Ndagi, U.; Mhlongo, N.; Soliman, M. E. Metal complexes in cancer therapy - an update from drug design perspective. *Drug Des., Dev. Ther.* **2017**, *11*, 599−616.
(14) Mjos, K. D.; Orvig, C. Metallodrugs in medicinal inorganic chemistry. *Chem. Rev.* **2014**, *114*, 4540−4563.
(15) Berners-Price, S. J.; Mirabelli, C. K.; Johnson, R. K.; Mattern, M. R.; McCabe, F. L.; Faucette, L. F.; Sung, C. M.; Mong, S. M.; Sadler, P. J.; Crooke, S. T. *In vivo* antitumor activity and *in vitro* cytotoxic properties of bis[1,2-bis(diphenylphosphino)ethane]gold(I) chloride. *Cancer Res.* **1986**, *46*, 5486−5493.
(16) Ssemaganda, A.; Low, L. M.; Verhoeft, K. R.; Wambuzi, M.; Kawoozo, B.; Nabasumba, S. B.; Mpendo, J.; Bagaya, B. S.; Kiwanuka, N.; Stanisic, D. I.; Berners-Price, S. J.; Good, M. F. Gold(I) phosphine compounds as parasite attenuating agents for malaria vaccine and drug development. *Metallomics* **2018**, *10*, 444−454.
(17) Glisic, B. D.; Djuran, M. I. Gold complexes as antimicrobial agents: An overview of different biological activities in relation to the

DOI: 10.1021/acs.jmedchem.9b01436
J. Med. Chem. 2020, 63, 2455−2469

oxidation state of the gold ion and the ligand structure. *Dalton Trans* **2014**, *43*, 5950−5969.
(18) Madeira, J. M.; Gibson, D. L.; Kean, W. F.; Klegeris, A. The biological activity of auranofin: Implications for novel treatment of diseases. *Inflammopharmacology* **2012**, *20*, 297−306.
(19) Fuchs, B. B.; RajaMuthiah, R.; Souza, A. C.; Eatemadpour, S.; Rossoni, R. D.; Santos, D. A.; Junqueira, J. C.; Rice, L. B.; Mylonakis, E. Inhibition of bacterial and fungal pathogens by the orphaned drug auranofin. *Future Med. Chem.* **2016**, *8*, 117−132.
(20) Aguinagalde, L.; Diez-Martinez, R.; Yuste, J.; Royo, I.; Gil, C.; Lasa, I.; Martin-Fontecha, M.; Marin-Ramos, N. I.; Ardanuy, C.; Linares, J.; Garcia, P.; Garcia, E.; Sanchez-Puelles, J. M. Auranofin efficacy against MDR *Streptococcus pneumoniae* and *Staphylococcus aureus* infections. *J. Antimicrob. Chemother.* **2015**, *70*, 2608−2617.
(21) AbdelKhalek, A.; Abutaleb, N. S.; Elmagarmid, K. A.; Seleem, M. N. Repurposing auranofin as an intestinal decolonizing agent for vancomycin-resistant *enterococci*. *Sci. Rep.* **2018**, *8*, 8353.
(22) Owings, J. P.; McNair, N. N.; Mui, Y. F.; Gustafsson, T. N.; Holmgren, A.; Contel, M.; Goldberg, J. B.; Mead, J. R. Auranofin and *N*-heterocyclic carbene gold-analogs are potent inhibitors of the bacteria *Helicobacter pylori*. *FEMS Microbiol. Lett.* **2016**, *363*, fnw148.
(23) Siles, S. A.; Srinivasan, A.; Pierce, C. G.; Lopez-Ribot, J. L.; Ramasubramanian, A. K. High-throughput screening of a collection of known pharmacologically active small compounds for identification of *Candida albicans* biofilm inhibitors. *Antimicrob. Agents Chemother.* **2013**, *57*, 3681−3687.
(24) Wiederhold, N. P.; Patterson, T. F.; Srinivasan, A.; Chaturvedi, A. K.; Fothergill, A. W.; Wormley, F. L.; Ramasubramanian, A. K.; Lopez-Ribot, J. L. Repurposing auranofin as an antifungal: *In vitro* activity against a variety of medically important fungi. *Virulence* **2017**, *8*, 138−142.
(25) Stylianou, M.; Kulesskiy, E.; Lopes, J. P.; Granlund, M.; Wennerberg, K.; Urban, C. F. Antifungal application of nonantifungal drugs. *Antimicrob. Agents Chemother.* **2014**, *58*, 1055−1062.
(26) Thangamani, S.; Maland, M.; Mohammad, H.; Pascuzzi, P. E.; Avramova, L.; Koehler, C. M.; Hazbun, T. R.; Seleem, M. N. Repurposing approach identifies auranofin with broad spectrum antifungal activity that targets Mia40-Erv1 pathway. *Front. Cell. Infect. Microbiol.* **2017**, *7*, 4.
(27) Diaz, R. S.; Shytaj, I. L.; Giron, L. B.; Obermaier, B.; della Libera, E.; Galinskas, J.; Dias, D.; Hunter, J.; Janini, M.; Gosuen, G.; Ferreira, P. A.; Sucupira, M. C.; Maricato, J.; Fackler, O.; Lusic, M.; Savarino, A.; SPARC Working Group.. Potential impact of the antirheumatic agent auranofin on proviral HIV-1 DNA in individuals under intensified antiretroviral therapy: Results from a randomized clinical trial. *Int. J. Antimicrob. Agents* **2019**, *54*, 592−600.
(28) Capparelli, E. V.; Bricker-Ford, R.; Rogers, M. J.; McKerrow, J. H.; Reed, S. L. Phase I clinical trial results of auranofin, a novel antiparasitic agent. *Antimicrob. Agents Chemother.* **2017**, *61*, e01947-16.
(29) Harbut, M. B.; Vilcheze, C.; Luo, X.; Hensler, M. E.; Guo, H.; Yang, B.; Chatterjee, A. K.; Nizet, V.; Jacobs, W. R., Jr.; Schultz, P. G.; Wang, F. Auranofin exerts broad-spectrum bactericidal activities by targeting thiol-redox homeostasis. *Proc. Natl. Acad. Sci. U. S. A.* **2015**, *112*, 4453−4458.
(30) Gandin, V.; Fernandes, A. P. Metal- and semimetal-containing inhibitors of thioredoxin reductase as anticancer agents. *Molecules* **2015**, *20*, 12732−12756.
(31) Thamban Chandrika, N.; Shrestha, S. K.; Ngo, H. X.; Howard, K. C.; Garneau-Tsodikova, S. Novel fluconazole derivatives with promising antifungal activity. *Bioorg. Med. Chem.* **2018**, *26*, 573−580.
(32) Thamban Chandrika, N.; Shrestha, S. K.; Ngo, H. X.; Tsodikov, O. V.; Howard, K. C.; Garneau-Tsodikova, S. Alkylated piperazines and piperazine-azole hybrids as antifungal agents. *J. Med. Chem.* **2018**, *61*, 158−173.
(33) Shrestha, S. K.; Garzan, A.; Garneau-Tsodikova, S. Novel alkylated azoles as potent antifungals. *Eur. J. Med. Chem.* **2017**, *133*, 309−318.
(34) Holbrook, S. Y. L.; Garzan, A.; Dennis, E. K.; Shrestha, S. K.; Garneau-Tsodikova, S. Repurposing antipsychotic drugs into antifungal agents: Synergistic combinations of azoles and bromperidol derivatives in the treatment of various fungal infections. *Eur. J. Med. Chem.* **2017**, *139*, 12−21.
(35) Shrestha, S. K.; Fosso, M. Y.; Garneau-Tsodikova, S. A combination approach to treating fungal infections. *Sci. Rep.* **2015**, *5*, 17070.
(36) Dennis, E. K.; Garneau-Tsodikova, S. Synergistic combinations of azoles and antihistamines against *Candida* species *in vitro*. *Med. Mycol.* **2019**, *57*, 874−884.
(37) Thamban Chandrika, N.; Dennis, E. K.; Shrestha, S. K.; Ngo, H. X.; Green, K. D.; Kwiatkowski, S.; Deaciuc, A. G.; Dwoskin, L. P.; Watt, D. S.; Garneau-Tsodikova, S. *N,N′*-Diaryl-bishydrazones in a biphenyl platform: Broad spectrum antifungal agents. *Eur. J. Med. Chem.* **2019**, *164*, 273−281.
(38) Fosso, M. Y.; Shrestha, S. K.; Thamban Chandrika, N.; Dennis, E. K.; Green, K. D.; Garneau-Tsodikova, S. Differential effects of linkers on the activity of amphiphilic tobramycin antifungals. *Molecules* **2018**, *23*, 899.
(39) Ngo, H. X.; Shrestha, S. K.; Garneau-Tsodikova, S. Identification of ebsulfur analogues with broad-spectrum antifungal activity. *ChemMedChem* **2016**, *11*, 1507−1516.
(40) Thamban Chandrika, N.; Shrestha, S. K.; Ngo, H. X.; Garneau-Tsodikova, S. Synthesis and investigation of novel benzimidazole derivatives as antifungal agents. *Bioorg. Med. Chem.* **2016**, *24*, 3680−3686.
(41) Shrestha, S. K.; Kril, L. M.; Green, K. D.; Kwiatkowski, S.; Sviripa, V. M.; Nickell, J. R.; Dwoskin, L. P.; Watt, D. S.; Garneau-Tsodikova, S. Bis(*N*-amidinohydrazones) and *N*-(amidino)-*N′*-aryl-bishydrazones: New classes of antibacterial/antifungal agents. *Bioorg. Med. Chem.* **2017**, *25*, 58−66.
(42) Gukathasan, S.; Parkin, S.; Awuah, S. G. Cyclometalated gold(III) complexes bearing DACH ligands. *Inorg. Chem.* **2019**, *58*, 9326−9340.
(43) Kim, J. H.; Reeder, E.; Parkin, S.; Awuah, S. G. Gold(I/III)-phosphine complexes as potent antiproliferative agents. *Sci. Rep.* **2019**, *9*, 12335.
(44) Uson, R.; Laguna, A.; Laguna, M.; Briggs, D. A.; Murray, H. H.; Fackler, J. P., Jr. (Tetrahydrothiophene)gold(I) or gold(III) Complexes. In *Inorganic Syntheses*; Kaesz, H. D., Ed.; Wiley, 1989; Vol. *26*, pp 85−91, DOI: 10.1002/9780470132579.ch17.
(45) Mohamed, A. A.; Krause Bauer, J. A.; Bruce, A. E.; Bruce, M. R. [Mu-*o*-phenylenebis(diphenylphosphine)-kappa^{2}P:P′]bis[chlorogold-(I)], dppbz(AuCl)$_2$. *Acta Crystallogr., Sect. C: Cryst. Struct. Commun.* **2003**, *59*, m84−86.
(46) Osawa, M.; Kawata, I.; Igawa, S.; Tsuboyama, A.; Hashizume, D.; Hoshino, M. Phosphorescence color alteration by changing counter anions on tetrahedral gold(I) complexes; intra- and interligand $\pi-\pi$ interactions. *Eur. J. Inorg. Chem.* **2009**, *2009*, 3708−3711.
(47) *CDC & FDA Antibiotic Resistance Isolate Bank*; CDC: Atlanta, GA.
(48) Costerton, J. W.; Stewart, P. S.; Greenberg, E. P. Bacterial biofilms: A common cause of persistent infections. *Science* **1999**, *284*, 1318−1322.
(49) Ciofu, O.; Rojo-Molinero, E.; Macia, M. D.; Oliver, A. Antibiotic treatment of biofilm infections. *APMIS* **2017**, *125*, 304−319.
(50) Percival, S. L.; Suleman, L.; Vuotto, C.; Donelli, G. Healthcare-associated infections, medical devices and biofilms: Risk, tolerance and control. *J. Med. Microbiol.* **2015**, *64*, 323−334.
(51) Costa-Orlandi, C. B.; Sardi, J. C. O.; Pitangui, N. S.; de Oliveira, H. C.; Scorzoni, L.; Galeane, M. C.; Medina-Alarcon, K. P.; Melo, W.; Marcelino, M. Y.; Braz, J. D.; Fusco-Almeida, A. M.; Mendes-Giannini, M. J. S. Fungal biofilms and polymicrobial diseases. *J. Fungi (Basel)* **2017**, *3*, 22.

DOI: 10.1021/acs.jmedchem.9b01436
J. Med. Chem. 2020, 63, 2455−2469

(52) Turan, H.; Demirbilek, M. Biofilm-forming capacity of bloodborne *Candida albicans* strains and effects of antifungal agents. *Rev. Argent. Microbiol.* **2018**, *50*, 62−69.
(53) Kojic, E. M.; Darouiche, R. O. *Candida* infections of medical devices. *Clin. Microbiol. Rev.* **2004**, *17*, 255−267.
(54) Nett, J.; Lincoln, L.; Marchillo, K.; Massey, R.; Holoyda, K.; Hoff, B.; VanHandel, M.; Andes, D. Putative role of beta-1,3 glucans in *Candida albicans* biofilm resistance. *Antimicrob. Agents Chemother.* **2007**, *51*, 510−520.
(55) Ramage, G.; Bachmann, S.; Patterson, T. F.; Wickes, B. L.; Lopez-Ribot, J. L. Investigation of multidrug efflux pumps in relation to fluconazole resistance in *Candida albicans* biofilms. *J. Antimicrob. Chemother.* **2002**, *49*, 973−980.
(56) Fiori, B.; Posteraro, B.; Torelli, R.; Tumbarello, M.; Perlin, D. S.; Fadda, G.; Sanguinetti, M. *In vitro* activities of anidulafungin and other antifungal agents against biofilms formed by clinical isolates of different *Candida* and *Aspergillus* species. *Antimicrob. Agents Chemother.* **2011**, *55*, 3031−3035.
(57) Dogan, I. S.; Sarac, S.; Sari, S.; Kart, D.; Essiz Gokhan, S.; Vural, I.; Dalkara, S. New azole derivatives showing antimicrobial effects and their mechanism of antifungal activity by molecular modeling studies. *Eur. J. Med. Chem.* **2017**, *130*, 124−138.
(58) Thamban Chandrika, N.; Shrestha, S. K.; Ranjan, N.; Sharma, A.; Arya, D. P.; Garneau-Tsodikova, S. New Application of neomycin B-bisbenzimidazole hybrids as antifungal agents. *ACS Infect. Dis.* **2018**, *4*, 196−207.
(59) Hasan, F.; Xess, I.; Wang, X.; Jain, N.; Fries, B. C. Biofilm formation in clinical *Candida* isolates and its association with virulence. *Microbes Infect.* **2009**, *11*, 753−761.
(60) Rodriguez-Cerdeira, C.; Gregorio, M. C.; Molares-Vila, A.; Lopez-Barcenas, A.; Fabbrocini, G.; Bardhi, B.; Sinani, A.; Sanchez-Blanco, E.; Arenas-Guzman, R.; Hernandez-Castro, R. Biofilms and vulvovaginal candidiasis. *Colloids Surf., B* **2019**, *174*, 110−125.
(61) Nett, J. E.; Andes, D. R. Fungal biofilms: *In vivo* models for discovery of anti-biofilm drugs. *Microbiol. Spectrum* **2015**, *3*, e30.
(62) Pongracz, J.; Benedek, K.; Juhasz, E.; Ivan, M.; Kristof, K. *In vitro* biofilm production of *Candida* bloodstream isolates: Any association with clinical characteristics? *J. Med. Microbiol.* **2016**, *65*, 272−277.
(63) Shin, J. H.; Kee, S. J.; Shin, M. G.; Kim, S. H.; Shin, D. H.; Lee, S. K.; Suh, S. P.; Ryang, D. W. Biofilm production by isolates of *Candida* species recovered from nonneutropenic patients: Comparison of bloodstream isolates with isolates from other sources. *J. Clin. Microbiol.* **2002**, *40*, 1244−1248.
(64) Tumbarello, M.; Posteraro, B.; Trecarichi, E. M.; Fiori, B.; Rossi, M.; Porta, R.; de Gaetano Donati, K.; La Sorda, M.; Spanu, T.; Fadda, G.; Cauda, R.; Sanguinetti, M. Biofilm production by *Candida* species and inadequate antifungal therapy as predictors of mortality for patients with candidemia. *J. Clin. Microbiol.* **2007**, *45*, 1843−1850.
(65) Wang, Y.; Liu, M.; Cao, R.; Zhang, W.; Yin, M.; Xiao, X.; Liu, Q.; Huang, N. A soluble bis-chelated gold(I) diphosphine compound with strong anticancer activity and low toxicity. *J. Med. Chem.* **2013**, *56*, 1455−1466.
(66) Jeswani, G.; Alexander, A.; Saraf, S.; Saraf, S.; Qureshi, A.; Ajazuddin. Recent approaches for reducing hemolytic activity of chemotherapeutic agents. *J. Controlled Release* **2015**, *211*, 10−21.
(67) Radwan, M. A.; AlQuadeib, B. T.; Siller, L.; Wright, M. C.; Horrocks, B. Oral administration of amphotericin B nanoparticles: Antifungal activity, bioavailability and toxicity in rats. *Drug Delivery* **2017**, *24*, 40−50.
(68) Uchida, M.; Sun, Y.; McDermott, G.; Knoechel, C.; Le Gros, M. A.; Parkinson, D.; Drubin, D. G.; Larabell, C. A. Quantitative analysis of yeast internal architecture using soft X-ray tomography. *Yeast* **2011**, *28*, 227−236.
(69) Fujioka, A.; Terai, K.; Itoh, R. E.; Aoki, K.; Nakamura, T.; Kuroda, S.; Nishida, E.; Matsuda, M. Dynamics of the Ras/ERK MAPK cascade as monitored by fluorescent probes. *J. Biol. Chem.* **2006**, *281*, 8917−8926.
(70) Mane, A.; Vidhate, P.; Kusro, C.; Waman, V.; Saxena, V.; Kulkarni-Kale, U.; Risbud, A. Molecular mechanisms associated with fluconazole resistance in clinical *Candida albicans* isolates from India. *Mycoses* **2016**, *59*, 93−100.
(71) Hargrove, T. Y.; Friggeri, L.; Wawrzak, Z.; Qi, A.; Hoekstra, W. J.; Schotzinger, R. J.; York, J. D.; Guengerich, F. P.; Lepesheva, G. I. Structural analyses of *Candida albicans* sterol 14alpha-demethylase complexed with azole drugs address the molecular basis of azole-mediated inhibition of fungal sterol biosynthesis. *J. Biol. Chem.* **2017**, *292*, 6728−6743.
(72) Franz, R.; Kelly, S. L.; Lamb, D. C.; Kelly, D. E.; Ruhnke, M.; Morschhauser, J. Multiple molecular mechanisms contribute to a stepwise development of fluconazole resistance in clinical *Candida albicans* strains. *Antimicrob. Agents Chemother.* **1998**, *42*, 3065−3072.
(73) Feng, W.; Yang, J.; Xi, Z.; Qiao, Z.; Lv, Y.; Wang, Y.; Ma, Y.; Wang, Y.; Cen, W. Mutations and/or overexpressions of *ERG4* and *ERG11* genes in clinical azoles-resistant isolates of *Candida albicans*. *Microb. Drug Resist.* **2017**, *23*, 563−570.
(74) Flowers, S. A.; Colon, B.; Whaley, S. G.; Schuler, M. A.; Rogers, P. D. Contribution of clinically derived mutations in ERG11 to azole resistance in *Candida albicans*. *Antimicrob. Agents Chemother.* **2015**, *59*, 450−460.
(75) Goldman, G. H.; da Silva Ferreira, M. E.; dos Reis Marques, E.; Savoldi, M.; Perlin, D.; Park, S.; Godoy Martinez, P. C.; Goldman, M. H.; Colombo, A. L. Evaluation of fluconazole resistance mechanisms in *Candida albicans* clinical isolates from HIV-infected patients in Brazil. *Diagn. Microbiol. Infect. Dis.* **2004**, *50*, 25−32.
(76) Teo, J. Q.; Lee, S. J.; Tan, A. L.; Lim, R. S.; Cai, Y.; Lim, T. P.; Kwa, A. L. Molecular mechanisms of azole resistance in *Candida* bloodstream isolates. *BMC Infect. Dis.* **2019**, *19*, 63.
(77) Rosana, Y.; Yasmon, A.; Lestari, D. C. Overexpression and mutation as a genetic mechanism of fluconazole resistance in *Candida albicans* isolated from human immunodeficiency virus patients in Indonesia. *J. Med. Microbiol.* **2015**, *64*, 1046−1052.
(78) Siikala, E.; Rautemaa, R.; Richardson, M.; Saxen, H.; Bowyer, P.; Sanglard, D. Persistent *Candida albicans* colonization and molecular mechanisms of azole resistance in autoimmune polyendocrinopathy-candidiasis-ectodermal dystrophy (APECED) patients. *J. Antimicrob. Chemother.* **2010**, *65*, 2505−2513.
(79) Mesa-Arango, A. C.; Rueda, C.; Roman, E.; Quintin, J.; Terron, M. C.; Luque, D.; Netea, M. G.; Pla, J.; Zaragoza, O. Cell wall changes in amphotericin B-resistant strains from *Candida tropicalis* and relationship with the immune responses elicited by the host. *Antimicrob. Agents Chemother.* **2016**, *60*, 2326−2335.
(80) Hebeka, E. K.; Solotorovsky, M. Development of resistance to polyene antibiotics in *Candida albicans*. *J. Bacteriol.* **1965**, *89*, 1533−1539.
(81) Gonzalez-Arellano, C.; Corma, A.; Iglesias, M.; Sanchez, F. Enantioselective hydrogenation of alkenes and imines by a gold catalyst. *Chem. Commun.* **2005**, 3451−3453.
(82) Krause, L.; Herbst-Irmer, R.; Sheldrick, G. M.; Stalke, D. Comparison of silver and molybdenum microfocus X-ray sources for single-crystal structure determination. *J. Appl. Crystallogr.* **2015**, *48*, 3−10.
(83) *APEX3*; Bruker-AXS Inc.: Madison, WI, U.S., 2016.
(84) Sheldrick, G. M. Crystal structure refinement with SHELXL. *Acta Crystallogr., Sect. C: Struct. Chem.* **2015**, *71*, 3−8.
(85) Sheldrick, G. M. SHELXT - integrated space-group and crystal-structure determination. *Acta Crystallogr., Sect. A: Found. Adv.* **2015**, *71*, 3−8.
(86) Spek, A. L. Structure validation in chemical crystallography. *Acta Crystallogr., Sect. D: Biol. Crystallogr.* **2009**, *65*, 148−155.
(87) Parkin, S. Expansion of scalar validation criteria to three dimensions: The R tensor. *Acta Crystallogr., Sect. A: Found. Crystallogr.* **2000**, *56*, 157−162.
(88) Clinical and Laboratory Standards Institute. *Reference method for broth dilution antifungal susceptibility testing of yeasts - Approved standard*. CLSI document M27-A3. Wayne, PA. 2008.

DOI: 10.1021/acs.jmedchem.9b01436
J. Med. Chem. 2020, 63, 2455−2469

(89) Clinical and Laboratory Standards Institute. *Reference method for broth dilution antifungal susceptibility testing of filamentous fungi - 2nd ed.*: CLSI document M38-A2. Wayne, PA. 2008.
(90) Klepser, M. E.; Malone, D.; Lewis, R. E.; Ernst, E. J.; Pfaller, M. A. Evaluation of voriconazole pharmacodynamics using time-kill methodology. *Antimicrob. Agents Chemother.* **2000**, *44*, 1917−1920.
(91) Pierce, C. G.; Uppuluri, P.; Tristan, A. R.; Wormley, F. L., Jr.; Mowat, E.; Ramage, G.; Lopez-Ribot, J. L. A simple and reproducible 96-well plate-based method for the formation of fungal biofilms and its application to antifungal susceptibility testing. *Nat. Protoc.* **2008**, *3*, 1494−1500.
(92) Nett, J. E.; Cain, M. T.; Crawford, K.; Andes, D. R. Optimizing a *Candida* biofilm microtiter plate model for measurement of antifungal susceptibility by tetrazolium salt assay. *J. Clin. Microbiol.* **2011**, *49*, 1426−1433.
(93) Lafleur, M. D.; Sun, L.; Lister, I.; Keating, J.; Nantel, A.; Long, L.; Ghannoum, M.; North, J.; Lee, R. E.; Coleman, K.; Dahl, T.; Lewis, K. Potentiation of azole antifungals by 2-adamantanamine. *Antimicrob. Agents Chemother.* **2013**, *57*, 3585−3592.
(94) Quave, C. L.; Estevez-Carmona, M.; Compadre, C. M.; Hobby, G.; Hendrickson, H.; Beenken, K. E.; Smeltzer, M. S. Ellagic acid derivatives from *Rubus ulmifolius* inhibit *Staphylococcus aureus* biofilm formation and improve response to antibiotics. *PLoS One* **2012**, *7*, e28737.
(95) Hall, B. S.; Bot, C.; Wilkinson, S. R. Nifurtimox activation by trypanosomal type I nitroreductases generates cytotoxic nitrile metabolites. *J. Biol. Chem.* **2011**, *286*, 13088−13095.
(96) Xu, W.; Zhu, X.; Tan, T.; Li, W.; Shan, A. Design of embedded-hybrid antimicrobial peptides with enhanced cell selectivity and anti-biofilm activity. *PLoS One* **2014**, *9*, e98935.
(97) Shrestha, S. K.; Fosso, M. Y.; Green, K. D.; Garneau-Tsodikova, S. Amphiphilic tobramycin analogues as antibacterial and antifungal agents. *Antimicrob. Agents Chemother.* **2015**, *59*, 4861−4869.
(98) Fosso, M. Y.; Shrestha, S. K.; Green, K. D.; Garneau-Tsodikova, S. Synthesis and bioactivities of kanamycin B-derived cationic amphiphiles. *J. Med. Chem.* **2015**, *58*, 9124−9132.
(99) Dartois, V.; Sanchez-Quesada, J.; Cabezas, E.; Chi, E.; Dubbelde, C.; Dunn, C.; Granja, J.; Gritzen, C.; Weinberger, D.; Ghadiri, M. R.; Parr, T. R., Jr. Systemic antibacterial activity of novel synthetic cyclic peptides. *Antimicrob. Agents Chemother.* **2005**, *49*, 3302−3310.
(100) Evans, B. C.; Nelson, C. E.; Yu, S. S.; Beavers, K. R.; Kim, A. J.; Li, H.; Nelson, H. M.; Giorgio, T. D.; Duvall, C. L. *Ex vivo* red blood cell hemolysis assay for the evaluation of pH-responsive endosomolytic agents for cytosolic delivery of biomacromolecular drugs. *J. Visualized Exp.* **2013**, e50166.
(101) Paderu, P.; Park, S.; Perlin, D. S. Caspofungin uptake is mediated by a high-affinity transporter in *Candida albicans*. *Antimicrob. Agents Chemother.* **2004**, *48*, 3845−3849.
(102) Zhang, W.; Cao, Y.; Gong, J.; Bao, X.; Chen, G.; Liu, W. Identification of residues important for substrate uptake in a glucose transporter from the filamentous fungus *Trichoderma reesei*. *Sci. Rep.* **2015**, *5*, 13829.

DOI: 10.1021/acs.jmedchem.9b01436
J. Med. Chem. 2020, 63, 2455−2469